BEST AVAILABLE IMAGES

Defective images within this document are accurate representations of the original documents submitted by the applicant.

Defects in the images may include (but are not limited to):

- BLACK BORDERS
- TEXT CUT OFF AT TOP, BOTTOM OR SIDES
- FADED TEXT
- ILLEGIBLE TEXT
- SKEWED/SLANTED IMAGES
- COLORED PHOTOS
- BLACK OR VERY BLACK AND WHITE DARK PHOTOS
- GRAY SCALE DOCUMENTS

IMAGES ARE BEST AVAILABLE COPY.

As rescanning documents *will not* correct images, please do not report the images to the Image Problem Mailbox.

REMARKS

In order to emphasize the patentable distinctions of applicants' invention over the prior art, claims 1, 12, and 36 have been amended to require that a surface on which a preselected contraband substance is to be detected is illuminated with infrared laser light of sufficient intensity and duration to cause selective ablation of molecules of the contraband surface. Support for the amendment of claims 1, 12, and 36 is found in the specification, e.g. at page 10, line 23; and page 17, line 13 to page 18, line 16. Consequently, no new matter has been added.

For the sake of clarity, claim 67 has been amended to recite a contraband agent that comprises an inorganic nitrate salt explosive agent. Support for the amendment to claim 67 is found in the specification, e.g. at page 26, lines 5 – 7. Consequently, no new matter has been added.

The present invention provides a versatile and efficient system for detecting a wide variety of contraband substances, notably including commonly used explosive agents. Such systems are now routinely used in many venues to protect the public from the obvious threat of terrorist acts entailing the use of explosives to damage or destroy airplanes and other public conveyances, public buildings, monuments, stadiums and arenas, and the like, whereby untold damage to life and property is inflicted. Advantageously, the present system permits the detection of minute residues of plastic explosives that are notoriously difficult to locate. Unlike previous systems that have required the use of direct mechanical contact with the object to be scrutinized, such as by a mechanical swabbing, the present system can accomplish its function remotely, employing laser ablation to remove sufficient

residue for analysis. Accordingly, the system can operate thoroughly and efficiently to scan items rapidly. Such functionality is highly beneficial in many public venues, such as airports, wherein large numbers of items must be scanned rapidly to preclude unacceptable delays, e.g. to travelers.

Claim 67 has been rejected under 35 USC 112, second paragraph. The Examiner has indicated that the term "said explosive agent" in line 1 lacks sufficient antecedent basis. As amended, claim 67 recites a method of detecting the presence of a preselected contraband substance on the surface of the object, the contraband substance being an inorganic nitrate explosive agent. The term "contraband substance" in amended claim 67 is submitted to find adequate antecedent basis in claim 12, from which claim 67 indirectly depends. In view of the amendment to claim 67, it is respectively submitted that claim 67 particularly points out and distinctly claims the subject matter regarded as the invention, thereby satisfying the statutory test.

Accordingly, reconsideration of the rejection under 35 USC 112, second paragraph, of claim 67 is respectfully requested.

Claims 1 – 3 have been rejected under 35 USC 102(e) as being anticipated by US Patent 5,416,321 to Sebastian et al., which discloses an apparatus which maps and detects contaminants within interior surfaces. The apparatus is said to include: (i) an optical vision system used to accurately map the surface to be investigated and treated and (ii) analytical probes used to sample the mapped surface to detect inorganic and organic contaminants in situ.

With respect to claim 1, the Examiner has pointed to col. 13, lines 20 – 62 which are alleged to disclose a method of removing a detectable portion of a pre-selected contraband

substance present on a surface, comprising illuminating said surface with light emitted from an infrared laser, said illumination having sufficient intensity and duration to cause selective desorption of molecules of said contraband substance without substantially damaging said surface.

Applicants respectfully traverse the contention that the Sebastian et al. disclosure reads on amended claim 1. In particular, Sebastian et al. discloses that vapors of the suspect substance are thermally desorbed and transported to a detector (see col. 13, lines 21 – 23). Applicants amended claims, on the other hand, require that a surface be illuminated with infrared laser light having sufficient intensity and duration to cause ablation of the suspect substance. One of ordinary skill in the art would recognize that ablation entails the removal of at least some particles of the substance, whereas thermal desorption of vapors as disclosed by Sebastian et al. entails only the removal of individual atoms or molecules of a substance. See, e.g., Leonid V. Zhigilei et al., "Molecular Dynamics Model for Laser Ablation and Desorption of Organic Solids," *J. Phys. Chem. B* 1997, *101*, pp. 2028-2037, especially at page 2028, first column, second paragraph, lines 5-10 and second column, second paragraph, lines 5-6; and Leonid V. Zhigilei et al., "Mesoscopic Breathing Sphere Model for Computer Simulation of Laser Ablation and Damage," Technical Proceedings 1999 International Conference on Modeling and Simulation of Microsystems (MSM '99), Applied Computational Research Society, 1999. Copies of these references are provided herewith for the Examiner's convenience.

It is respectfully submitted that Sebastian et al. does not disclose or suggest any illumination that results in ablation, and rather teaches away from ablation in favor of thermal desorption. Such a process is far less efficient in removing material and produces a

far smaller mass of analyte that is also more dilute in the transporting gas, e.g. the air stream provided by the blower described at col. 13, lines 33 – 35. Moreover, applicants respectfully submit that Sebastian et al. expressly teaches away from any process that entails removal of material from the surface being analyzed. See, e.g., col. 8, lines 26 – 28, and col. 14, lines 68 – 68. Applicants thus maintain that Sebastian et al. fails to disclose every feature of amended claim 1, as required for a rejection under 35 USC 102(e).

With respect to claim 2, Sebastian et al. is said to disclose the use of a continuous infrared beam at col. 10, lines 48 – 52. With respect to claim 3, the Examiner indicates that Sebastian et al. at col. 14, lines 14 – 19 discloses a method wherein the infrared laser emits pulses of infrared light. As set forth above in connection with the rejection of claim 1 under 35 USC 102(e), Sebastian et al. does not disclose laser ablation of a sample, and thus fails to teach all the features of present claim 1, from which claims 2 – 3 depend. Applicants thus submit that claims 2 and 3, being dependent from amended claim 1, are patentable for at least the same reasons. Moreover, applicants submit that col. 14, lines 14 – 19 does not support the Examiner's position that Sebastian et al. discloses a pulsed infrared laser beam. In particular, the pulses are said to be generated within a conventional time-of-flight mass spectrometer (TOF-MS) (lines 10-11). The cited text clearly indicates that the pulse extracts ion from the ion source (lines 15 – 16), not from any surface from which suspect contraband material is being removed for analysis. Nor is their any indication that the extraction pulse is a light pulse. Applicants thus maintain that the Examiner has not established any case of prima facie anticipation by Sebastian et al. with respect to amended claims 1 – 3.

Accordingly, reconsideration of the rejection under 35 USC 102(e) of amended claims 1 – 3 as being anticipated by Sebastian et al. is respectfully requested.

Claims 4 – 6 have been rejected under 35 USC 103(a) as being unpatentable over Sebastian et al.

The Examiner has indicated that Sebastian et al. discloses the claimed invention except for the actual specific pulse repletion rate, and spot size (spot focusing) data, and that it would have been obvious to one of ordinary skill to experimentally adjust the lasing and laser beam parameters, it having been held that the provision of adjustability, where needed, involves only routine skill in the art. Sebastian et al. is said to disclose a pulse duration of 100 μs (col. 14, lines 17 – 19).

Although the Examiner has not provided any specific authority concerning adjustability on which this rejection is based, applicants infer that he has in view the discussion of adjustability at MPEP 2144.04V-D, which relies on ***In re Stevens***, 41 C.C.P.A. 864, 212 F.2d. 197 (1954). Applicants respectfully submit that the facts of ***Stevens*** are inapposite in the present instance. The ***Stevens*** invention is directed to a handle for a fishing rod wherein: (i) an adjustment permits selection of the angle of a hand grip relative to the axial disposition of the rod and (ii) a grip for a finger of the hand grasping the hand grip is carried by an elongated reel-supporting body between the ends thereof and longitudinally adjustably. *Id.* at 865. Significantly, a prior art reference, U.S. Patent 2,000,263 to Teetor, cited during the prosecution of the patent at issue discloses a fishing rod with a handle that may be located either in a position that constitutes substantially an elongation of the rod (said to be a convenient casting position) or shifted to a position that is downwardly inclined with respect to the rod, after the manner of a pistol

grip (said to be convenient for trolling). The C.C.P.A. affirmed the reasoning of the Board of Appeals that if desirable, the Teetor fishing rod could be provided with a universal connection, whereby the relative angular positioning of the grip and the rod could be adjusted to a plurality of positions, and not merely the two positions disclosed by Teetor. Moreover, the Court noted that: "Of course, the need for adjustment in a fishing rod is something, according to the record, that has long been recognized as desirable for the reason that some fishermen like to see what particular angle best suits their own hands and their method of casting." *Id.* at 866.

In the present instance, the Examiner has not pointed to any disclosure or suggestion in the prior art of the need or desirability of adjusting the pulse duration, pulse repetition rate, or laser spot size for a laser used in a method of removing, by ablation, a detectable portion of a pre-selected contraband substance present on a surface. While such adjustments are admittedly known for lasers used in other contexts, no art has been adduced that suggests that the adjustments are needed or desired for lasers used in contraband detection systems. Even less is there any disclosure or suggested in the cited art of any specific pulse durations, pulse repetition rates, or spot size, let alone the particular numerical values delineated by instant claims 4 – 6. Applicants respectfully submit that the reasoning in ***Stevens*** requires evidence in the art of a known need or desirability for adjustment. In the present instance, there is no such evidence of record. In addition, the adjustment held to be unpatentable in ***Stevens*** was an adjustment intermediate extreme limits expressly disclosed for the Teetor fishing rod. The Examiner has not pointed to any disclosure or suggestion of known laser ablation systems for removing contraband substances for analysis wherein the laser light satisfies any of the limits set forth in claims

4 – 6. The Examiner's own statement ("... adjustability, when needed..." page 4, paragraph 4, emphasis added) points to the lack of pertinence of ***Stevens***, since no desirability, let alone need, as been demonstrated. Accordingly, it is submitted that one of ordinary skill in the art would have no motivation for selection or adjustment of the recited laser characteristics. Inasmuch as no ranges or particular values of any of the recited characteristics disclosed or suggested by the art of record, selection of values within these ranges cannot be regarded as an adjustment between known limits, as required for ***Stevens*** to be pertinent.

Furthermore, none of claims 4 – 6 requires adjustability, as also would be essential for ***Stevens*** to be pertinent. Rather, claims 4 – 6 set forth ranges relating to characteristics of the laser used in the present method that are preferred for accomplishing the laser ablation recited by amended claim 1, from which claims 4 – 6 depend. Inasmuch as the Examiner has not pointed to any disclosure or suggestion in Sebastian et al. of laser ablation, selection of laser parameters such as those delineated by claims 4 – 6 cannot be regarded as "adjustment."

While the Examiner points to col. 14, lines 17 – 19 as disclosing a pulse duration of 100 μs, it is submitted that this duration is not a duration of any laser light pulse impinging on a surface being scrutinized. Rather, as discussed hereinabove in connection with the rejection of claim 3 under 35 USC 102(e), the 100 μs referenced is said to be a duration between extraction pulses (line 19). Such pulses are generated within a conventional time-of-flight mass spectrometer (TOF-MS) (lines 10-11). The cited text clearly indicates that the pulse extracts ion from the ion source (lines 15 – 16), not from any surface from which

suspect contraband material is being removed for analysis. Nor is their any indication that the extraction pulse is a light pulse.

Accordingly, reconsideration of the rejection under 35 USC 103(a) of claims 4 – 6 as being unpatentable over Sebastian et al. is respectfully requested.

Claims 7 – 8 have been rejected under 35 USC 103(a) as being unpatentable over Sebastian et al. in view of US Patent 5,241,179 to Carrieri.

Carrieri discloses a system for remotely detecting liquid contaminants on surfaces, including chemical agents and their simulants. The system is said to include a Fourier Transform Infrared Spectroradiometer aligned to optionally develop graybody photoluminescence spectra from the generation of a plurality of interferograms co-added to provide a favorable signal to noise ration. A laser is used for surface irradiating a substrate potentially having the chemical agents to heat the substrate.

As set forth hereinabove in connection with the rejection under 35 USC 102(e) of claims 1 – 3 over Sebastian et al., applicants respectfully submit that Sebastian et al. fails to disclose or suggest any method in which a suspect sample is ablated from a surface being scrutinized. Carreri does not cure this deficiency. As a result, claims 7 – 8, which depend from claim 1, are also submitted to be patentable.

The Examiner correctly acknowledges that Sebastian et al. fails to disclose use of a CO_2 laser employing isotopically CO_2 enriched gas, but indicates that Carrieri shows that it is known to provide a CO_2 isotopically enriched laser for a thermoluminescence sensor. He indicates that it would have been obvious to one of ordinary skill in the art to combine the device of Sebastian with the CO_2 isotopically enriched laser of Carrieri for the purpose of producing a photoluminescent signal from the substrate to be analyzed.

Applicants respectfully submit that Carrieri in fact teaches away from the present invention, in that the photoluminescent signal on which the Carrieri apparatus requires that sample be present on the surface, instead of being removed therefrom, as delineated by the method recited by present claim 1. Moreover, Carrieri's use of an isotopically enriched laser is submitted to be for a purpose that is unrelated to applicants' system. The motivation for the Examiner's proposed combination is said to be for the purpose of producing a photoluminescent signal from the substrate. The isotopically enriched laser is said to provide an enhanced signal. By way of contrast, the method called for by applicants' claims does not employ a photoluminescent signal from the substrate. Instead, applicants' laser acts to cause ablation of sample from the surface. The ablated sample is then analyzed separately. Significantly, Carrieri provides no disclosure or suggestion of ablation or other form of sample removal as the result of the impingement of laser light, let alone an enhancement of sample removal attendant to the use of an isotopically enriched CO_2 laser.

Accordingly, reconsideration of the rejection of claims 7 – 8 under 35 USC 103(a) as being obvious over the combination of Sebastian et al. and Carrieri is respectfully requested.

Claims 9 – 20, 23 – 43, 46 – 66, and 68 have been rejected under 35 USC 103(a) as being unpatentable over Sebastian et al. in view of US Patent 6,610,977 to Megerle.

Megerle provides a method and apparatus for screening an object for the presence of an explosive, chemical warfare agent, and/or radioactive material. The apparatus includes a portal through which the object is arranged to pass. The portal comprises a housing having

an ion mobility spectrometer and a surface acoustic wave device for detecting explosives, drugs, and chemical warfare agents.

With respect to claims 9 – 11, the Examiner states that the Megerle abstract shows that it is known to provide a contraband substance comprising an explosive, a narcotic, or a chemical agent for a security system and that it would have been obvious to someone of ordinary skill to combine the device of Sebastian et al. with the security system for detecting an explosive, a narcotic, or a chemical agent of Megerle for the purposes of providing protection from outside threats.

As set forth hereinabove in connection with the rejection under 35 USC 102(e) of claims 1 – 3 over Sebastian et al., applicants respectfully submit that Sebastian et al. fails to disclose or suggest any method in which a suspect sample is ablated from a surface being scrutinized. Megerle does not cure this deficiency. At best, Megerle suggests that particles be dislodged from a person or object by impingement of air streams. No suggestion is made of any form of illumination of the person or object to be analyzed, let alone illumination by a laser that results in ablation of suspect substances. Accordingly, it is submitted that claims 9 – 11, which depend from claim 1, are patentable over the combination of Sebastian et al. and Megerle for at least the same reasons as claim 1.

The ablation feature recited in claim 1 is similarly recited in amended claim 12 (and claims 13 – 20, 23 – 35 dependent thereon) and amended claim 36 (and claims 37 – 68 dependent thereon). As a result, claims 12 – 20, 23 – 43, 46 – 66, and 68 are also submitted to be patentable over the combination of Sebastian et al. and Megerle for at least the reasons set forth hereinabove in connection with the 102(e) rejection of claim 1 – 3

over Sebastian et al. and the 103(a) rejection of claims 9 – 11 over the combination of Sebastian et al. and Megerle.

With respect to claim 12, the Examiner has indicated that Sebastian et al substantially teaches the claimed invention. Acknowledging that Sebastian et al. fails to teach the outputting of an electrical signal representative of the presence of the contraband substance and the activating of a signal means in response to the electrical signal, he points to Megerle. However, as discussed more fully above, applicants traverse the Examiner's contention that Sebastian et al. substantially teaches the features delineated by claim 12, particularly including laser ablation. Therefore, it is submitted that the combination of Sebastian et al. and Megerle fails to disclose or suggest every feature of amended claim 12.

With respect to claims 13 and 14, the Examiner has indicated that Sebastian et al. in view of Megerle discloses the use of a continuous or pulsed beam. The citations given are apparently to the Sebastian et al. patent. As set forth in connection with the rejection of claims 1 – 3, applicants respectfully submit that Sebastian et al. does not disclose or suggest any method in which a laser is used to ablate sample for analysis, let alone the particular method recited by claims 13 – 15. The particular passages in Sebastian cited are submitted not to be relevant. Col. 10, lines 48 – 52 are directed to an optical vision system employing a continuous laser, while the discussion at col. 14, lines 17 – 19 is nowhere stated to entail laser or other optical pulses. Neither passage discloses or suggests the use of any laser to effect ablation. Applicants are likewise unable to locate any reference in Megerle of illuminating a sample to ablate material for analysis, and the Examiner has not pointed to any such reference.

With respect to claim 15, the Examiner alleges that one of ordinary skill would find it obvious that most lasers are continuous and that some form of shutter (chopper) is required in order to create a pulsed beam of light. Accordingly, he indicates that the pulsed laser of Sebastian et al. in view of Megerle is created using a shutter (chopper) to create a pulsed effect.

Applicants respectfully traverse these indications. As set forth above, the citation in Sebastian et al. that the Examiner has furnished is not directed to any pulsed laser or other optical beam. Even if it were, applicants further traverse the contention that it is inherent that a pulsed laser employs a shutter or chopper.

The Board of Patent Appeals and Interferences has ruled that "when an examiner relies on inherency, it is incumbent on the examiner to point to the *'page and line'* of the prior art which justifies an inherency theory." ***Ex parte Schricker***, 56 USPQ 2d 1723, 1725 (B.P.A.I. 2000) (unpublished), quoting ***In re Rijckaert***, 9 F.3d 1531, 1533, 28 USPQ 2d 1955, 1957 (Fed. Cir. 1993) and ***In re Yates***, 663 F.2d 1054, 1057, 211 USPQ 1149, 1151 (C.C.P.A. 1981). In the present instance, the Examiner has not provided such specificity. Moreover, applicants respectfully traverse the purported inherency. From the earliest days of laser technology, pulsed lasers not involving shutters have been known, such lasers being activated by other means, e.g. by pulses of light from a gas-filled flash lamp. See, e.g., U.S. Patent 3,353,115 to T.H. Maiman, e.g. at col. 8, lines 44 – 46 and Fig. 18. Applicants respectfully request that the Examiner either provide a reference to support the alleged inherency or withdraw the rejection of claim 15. Applicants further submit that the reasons set forth in connection with the rejection of claims 13 – 14 apply with equal force to claim 15.

With respect to claim 16, the Examiner has indicated that Sebastian et al. in view of Megerle discloses a method wherein an infrared laser emits pulses of infrared light. As set forth hereinabove in connection with the rejection of claim 3 under 35 USC 102(e), applicants respectfully submits that Sebastian et al. in fact does not disclose or suggest a pulsed laser.

With respect to claims 17, 18, 19, and 20, the Examiner indicated that Sebastian et al. discloses the claimed invention except for the specific pulse repletion rate, spot size, and fluence and that it would have been obvious to one having ordinary skill to experimentally adjust the lasing and laser beam parameters, since it has been held that the provision of adjustability, where needed, involves only routine skill in the art. Sebastian et al is said to disclose a pulse duration of 100 μs.

For at least the reasons set forth hereinabove in connection with the rejection of claims 4 – 6 under 35 USC 103(a), applicants respectfully traverses the Examiner's contention. Claims 17 – 20 are submitted not to require the adjustability that the Examiner has indicated. In addition, it is submitted that the Examiner has not pointed to any disclosure or suggestion of the particular conditions delineated by claims 17 – 20, or any motivation for an artisan to make the selections recited therein. As also noted above, the 100 μs referenced in the cited passage at col. 14, lines 17 – 19 is not directed to any laser pulse duration.

With respect to claims 23 – 26, the Examiner has indicated that Sebastian et al. substantially teaches the claimed invention, except for a failure to show a contraband substance comprising an explosive, an organo-nitro explosive, a narcotic, or a chemical agent. Accordingly, he has pointed to Megerle as disclosing these features.

As set forth hereinabove, applicants respectfully submit that Sebastian et al. and Megerle, whether taken singly or in combination, fails to disclose a method in which a laser is used to ablate molecules of a contraband substance for analysis. While Megerle admittedly provides a system by which objects may be screened for the presence of various substances, e.g. explosives, the Megerle system accomplishes such an objective by an entirely different means that does not entail laser ablation, as required by present claim 12, from which claims 23 – 26 depend. Applicants thus maintain that the combination of Sebastian et al. and Megerle does not disclose or suggest the subject matter delineated by present claims 23 – 26.

With respect to claims 27 – 29, the Examiner has taken official notice that pyrolysis, GC/IMS, and surface ionization detectors are common detectors in the field of contraband detection. This knowledge, in combination with the Sebastian et al. and Megerle disclosures is said to read on claims 27 – 29. Applicants respectfully disagree, inasmuch as the combination of Sebastian et al. and Megerle fails to disclose the laser ablation required by amended claim 12, from which claims 27 – 29 depend.

With respect to claims 30 – 34, the Examiner has pointed to various disclosures in Sebastian et al. and Megerle regarding the motion of the light beam and the object being scrutinized and has indicated that these disclosures render obvious the subject matter of claims 30 – 34. As set forth above in connection with the rejection of claims 9 – 11 under 35 USC 103(a), the feature of laser ablation is not disclosed or suggested even by the combination of Sebastian et al. and Megerle. Such feature is also required by amended claim 12, from which claims 30 – 34 depend directly or indirectly. Accordingly, it is

submitted that the combination of Sebastian et al. and Megerle fails to disclose or suggest all the features of present claims 30 – 34, as is required for a 103(a) rejection.

With respect to claim 35, the Examiner indicates that Sebastian et al. in view of Megerle discloses a method comprising displaying a mapping on a computer display terminal, the mapping being indicative of locations at which a contraband substance has been detected. As set forth hereinabove in connection with the rejection of claims 1 – 3 under 35 USC 102(e) and of claims 4 – 6 and claim 12 (from which claim 35 depends) under 35 USC 103(a), applicants maintain that even in combination, Sebastian et al. and Megerle fail to disclose or suggest the laser ablation feature required by amended claim 12, from which claim 35 depends. Accordingly, claim 35 is submitted to be patentable over Sebastian et al. and Megerle for at least the same reasons as claim 12.

With respect to claim 36, the Examiner has indicated that Sebastian et al. discloses an apparatus for nondestructively detecting the presence of a contraband substance on the surface of an object and that Megerle shows that it is known to provide an electrical signal responsive to the detection of the contraband substance, the signal activating a signal means. However, as set forth hereinabove in connection with the rejection of claims 1 – 3 under 35 USC 102(e) and of claims 4 – 6 and claim 12 (from which claim 35 depends) under 35 USC 103(a), applicants maintain that even in combination, Sebastian et al. and Megerle fail to disclose or suggest an apparatus in which an infrared laser is used to illuminate an interrogation area of a surface, the illumination having sufficient intensity and duration to cause selective ablation of molecules of the contraband surface, as required by feature (b) of amended claim 36. Accordingly, it is submitted that Sebastian et al. and

Megerle fail to disclose or suggest every feature of claim 36, as required for a rejection under 35 USC 103(a).

With respect to claims 37 – 40, the Examiner has indicated that Sebastian et al. in view of Megerle discloses the use of a continuous infrared beam and a pulsed infrared beam. Applicants respectfully disagree, for the reasons set forth in connection with the rejection of method claims 13 – 15. In particular, applicants respectfully submit that Sebastian et al. does not disclose or suggest any apparatus in which a laser is used to ablate sample for analysis, let alone the particular apparatus recited by claims 37 – 40. The particular passages in Sebastian cited are submitted not to be relevant. Col. 10, lines 48 – 52 are directed to an optical vision system employing a continuous laser, while the discussion at col. 14, lines 17 – 19 is nowhere stated to entail laser or other optical pulses. Neither passage discloses or suggests the use of any laser to effect ablation. Applicants are likewise unable to locate any reference in Megerle of illuminating a sample to ablate material for analysis, and the Examiner has not pointed to any such reference.

Further with respect to claim 39, applicants traverse the Examiner's reliance on an inherency argument, as discussed more fully in connection with the rejection of claim 15 above.

With respect to claims 41 – 43, the Examiner has indicated that Sebastian et al. discloses the claimed apparatus except for particular details of pulse repetition rate and spot size and that it would be obvious to experimentally adjust the lasing and laser beam parameters. Applicants' discussion hereinabove in connection with the rejection of claims 4 – 6 and 17 – 20 under 35 USC 103(a) is submitted to apply with equal force to claims 41 – 43. In particular, applicants maintain that claims 41 – 43 do not require the adjustability

imputed thereto by the Examiner, nor is there any disclosure of the particular laser characteristics recited by the claims. Sebastian et al. and Megerle both fail to recognize any process or apparatus entailing laser ablation of a contraband substance on a surface. Hence there is no motivation for selection of particular preferred laser characteristics for accomplishing the ablation delineated by claim 36, from which claims 41 – 43 depend indirectly. Accordingly, claims 41 – 43 are submitted to be patentably unobvious over Sebastian et al. and Megerle.

With respect to claims 46 – 49, the Examiner has indicated that Sebastian et al. substantially teaches the claimed invention, except for the identification of the contraband substance as comprising an explosive, an organo-nitro explosive compound or inorganic nitrate salt, a narcotic, or a chemical agent. As also set forth hereinabove in connection with the rejection of claims 23 – 26 under 35 USC 103(a), applicants respectfully submit that the combination of Sebastian et al. and Megerle fails to disclose or suggest any apparatus wherein ablation of material from a surface is effected by illumination by an infrared laser. Inasmuch as this feature is delineated by proviso (b) of amended claim 36, from which claims 46 – 49 depend indirectly, it is submitted that not all the features of claims 46 – 49 are disclosed or suggested by the combination of Sebastian et al. and Megerle. Accordingly, applicants maintain that claims 46 – 49 should not be subject to rejection over said references.

With respect to claims 50 – 52, the Examiner has taken official notice that pyrolysis, GC/IMS, and surface ionization detectors are common detectors in the field of contraband detection. This knowledge, in combination with the Sebastian et al. and Megerle disclosures is said to read on claims 50 – 52. Applicants respectfully disagree, inasmuch as

the combination of Sebastian et al. and Megerle fails to disclose any apparatus comprising a laser adapted to illuminate a surface with sufficient intensity and duration to cause selective ablation of molecules of a contraband substance, as required by amended claim 36, from which claims 50 – 52 depend indirectly.

With respect to claims 53 – 58, the Examiner has pointed to various disclosures in Sebastian et al. and Megerle regarding the motion of the light beam and the object being scrutinized and has indicated that these disclosures render obvious the subject matter of claims 53 – 58. As set forth above in connection with the rejection of claims 9 – 11 and corresponding method claims 30 – 34 under 35 USC 103(a), the feature of laser ablation is not disclosed or suggested even by the combination of Sebastian et al. and Megerle. Such feature is also required by amended claim 36, from which claims 53 – 58 depend directly or indirectly. Accordingly, it is submitted that the combination of Sebastian et al. and Megerle fails to disclose or suggest all the features of present claims 53 – 58, as is required for a 103(a) rejection.

With respect to claim 58, the Examiner indicates that Sebastian et al. in view of Megerle discloses a method comprising displaying a mapping on a computer display terminal, the mapping being indicative of locations at which a contraband substance has been detected. As set forth hereinabove in connection with the rejection of claims 1 – 3 under 35 USC 102(e) and of claims 4 – 6, 12, and 36 under 35 USC 103(a), applicants maintain that even in combination, Sebastian et al. and Megerle fail to disclose or suggest the laser ablation feature required by amended claim 36, from which claim 58 depends. Accordingly, claim 58 is submitted to be patentable over Sebastian et al. and Megerle for at least the same reasons as claim 36.

With respect to claims 59 and 61, the Examiner has indicated that it is obvious to one of ordinary skill that the intensity and duration of illumination should not be sufficient to cause substantial deflagration or detonation of an explosive system in order to insure the safety of those performing the analysis. Applicants respectfully traverse the basis on which the Examiner has made this rejection. It is well known to those of ordinary skill in the art that persons handling many common forms of explosives, notably including plastic explosives such as C-4 and SEMTEX, pick up minute residues on their hands which are frequently transferred to the surface of objects they subsequently handle. The amount of residual explosive in these circumstances is generally so minute that there is little or no chance of harm coming to any person as a result of detonation of the residue, yet it is this residue that the present apparatus is capable of detecting. Moreover, as set forth in the present specification at page 7, lines 3 – 13, detection systems employing intentionally induced, selective deflagration or micro-detonations of explosive residues on the surface of an article have been proposed. Such reactions are said to produce a detectable optical signature by which the presence of the explosives is indicated, thereby teaching away from the Examiner's position. Clearly, persons contemplating such a system do not regard the Examiner's concerns regarding safety as determinative. See, e.g., US Patent 5,760,898 to Haley et al., which discloses a detection system that employs the optical characteristics of surface micro-detonations for detection. In addition, as set forth in the specification at page 8, lines 21 – 23, leaving a detectable residue of the suspect material on the object permits further examination and/or additional analytic tests at a future point. The possibility of such testing is of importance in some instances, e.g. in situations where follow-up forensic evidence is sought by law enforcement or other authorities.

With respect to claims 60 and 62, the Examiner has pointed to Megerle's disclosure of detecting plastic explosives. However, as set forth above, the combination of Sebastian et al. and Megerle fails to disclose any apparatus comprising a laser and illumination therefrom that results in ablation of contraband sample, as recited by claim 36, as amended. Accordingly, claims 60 and 62 (which depend directly or indirectly from amended claim 36) are submitted to be patentably unobvious.

With respect to claims 63 – 66, the Examiner has taken official notice that FIS, gas-phase infrared, and photo acoustic detectors are known in the field of contraband detection. Sebastian et al. in view of Megerle was thus said to read on the claimed limitations. As set forth in connection of the foregoing discussion of claims 27 – 29 and 50 – 52 in which similar official notice was taken, applicants respectfully maintain that the laser ablation feature of amended claim 36, on which claims 63 – 66 depend, is not disclosed or suggested by the combination of Sebastian et al. and Megerle. Accordingly, it is submitted that claims 63 – 66 are patentable over Sebastian et al. and Megerle.

With respect to claim 68, the Examiner has pointed to the inclusion of an inorganic nitrate salt in the List of Explosive Materials disclosed by Megerle. Applicants again maintain that the combination of Sebastian et al. and Megerle fails to disclose or suggest the laser ablation feature delineated by amended claim 36, from which claim 68 indirectly depends.

Accordingly, reconsideration of the rejection under 35 USC 103(a) of claims 9 – 20, 23 – 43, 36 – 66, and 68 over Sebastian et al. in view of Megerle is respectfully requested.

Claims 21, 22, 44, and 45 have been rejected under 35 USC 103(a) as being unpatentable over Sebastian et al. in view of Megerle and further in view of Carrieri.

Carrieri is said to provide a CO_2, isotopically enriched laser known for a thermoluminescence sensor. It is indicated that it would have been obvious to one of ordinary skill to combine the device of Sebastian et al. in view of Megerle with the laser of Carrieri for the purpose of producing a photoluminescent signal from the substrate being analyzed.

As also set forth hereinabove in connection with the rejection of claims 7 – 8 under 35 USC 103(a), applicants respectfully submit that Carrieri in fact teaches away from the present invention, in that the photoluminescent signal on which the Carrieri apparatus requires that sample be present on the surface, instead of being removed therefrom, as delineated by the method recited by claims 21 and 22 and the apparatus recited by claims 44 and 45. Moreover, Carrieri's use of an isotopically enriched laser is submitted to be for a purpose that is unrelated to applicants' system. The motivation for the Examiner's proposed combination is said to be for the purpose of producing a photoluminescent signal from the substrate. By way of contrast, applicants' method does not employ a photoluminescent signal from the substrate. Instead, applicants' laser acts to cause ablation of sample from the surface. The ablated sample is then analyzed separately. Significantly, Carrieri provides no disclosure or suggestion of ablation or other form of sample removal as the result of the impingement of laser light, let alone an enhancement of sample removal attendant to the use of an isotopically enriched CO_2 laser.

Accordingly, reconsideration of the rejection under 35 USC 103(a) of claims 21, 22, 44, and 45 over Sebastian et al. in view of Megerle and further in view of Carrieri is respectfully requested.

In view of the amendments to claims 1, 12, 36, and 67, and the foregoing remarks, it is respectfully submitted that the present application has been placed in allowable condition. Reconsideration of the rejection of claims 1 – 68, as amended, and allowance of the present application, are, therefore, earnestly solicited.

Respectfully submitted,

Dao Hinh Nguyen et al

By
Ernest D. Buff
(Their Attorney)
Reg. No. 25,833
(973) 644-0008

Molecular Dynamics Model for Laser Ablation and Desorption of Organic Solids

Leonid V. Zhigilei, Prasad B. S. Kodali, and Barbara J. Garrison*

Department of Chemistry, 152 Davey Laboratory, The Pennsylvania State University, University Park, Pennsylvania 16802

Received: October 31, 1996; In Final Form: January 14, 1997[⊗]

A breathing sphere model is developed for molecular dynamics simulations of laser ablation and desorption of organic solids. An approximate representation of the internal molecular motion permits a significant expansion of the time and length scales of the model and still allows one to reproduce a realistic rate of the vibrational relaxation of excited molecules. We find that the model provides a plausible description of the ablation of molecular films and matrix-assisted laser desorption. An apparent threshold fluence has been found to separate two mechanisms for the ejection of molecules: surface vaporization at low laser fluences and collective ejection or ablation at high fluences. Above threshold the laser-induced high pressure and the explosive homogeneous phase transition lead to the strongly forwarded emission of ablated material and high, from 500 up to 1500 m/s, maximum velocities of the ejected plume expansion. Large analyte molecules get axial acceleration from an expanding plume and move along with the matrix molecules at nearly the same velocities. Big molecular clusters are found to constitute a significant part of the ejected plume at fluences right above the ablation threshold. The processes in the plume are found to have a strong influence on the final velocities of ejected molecules and molecular clusters.

I. Introduction

Laser ablation of organic solids is a process with a wide range of practical applications. In surgery, this process is used for controlled removal of tissue, and scientific and technological efforts are aimed at achieving more precise control over the ablation depth and minimizing thermal and mechanical damage.[1] In mass spectrometry laser ablation is used to produce big nonvolatile organic molecules or ions in the gas phase for subsequent mass-spectrometric investigations.[2] Recent developments of the matrix-assisted laser desorption ionization (MALDI) technique have dramatically increased the available mass range and possible resolution.[3,4] In this situation the molecules of interest (i.e. the analytes) are incorporated into a matrix of molecules that readily absorb the incident laser light.

Despite an active practical use of laser ablation and extensive experimental[5−14] and theoretical[15−22] studies, the understanding of the underlying elementary processes is rather poor and optimum values of the experimental parameters are arrived at empirically. The complexity and diversity of the processes involved in laser ablation, namely, laser excitation of absorbing molecules, energy transfer from the excited molecules into the internal and translational modes of the solid, material disintegration, and prompt forward ejection along with processes in the plume, hinder the analytical description of the phenomenon. Even a qualitative picture of laser ablation has not been established, and analytical models based on such diverse assumptions as the thermofluctuational sublimation of molecules from the surface (surface vaporization)[9,17] and explosive bulk desorption due to a nonequilibrium phase transition[7,16] or critical pressure gradient[14,15,21,22] are used to explain the experimental observations.

In the situation where the analytical description of the laser ablation of organic solids is hindered by the complexity and diversity of the processes involved in the phenomenon, an analysis based on the molecular dynamics (MD) computer simulation technique can provide useful information. The advantage of this approach is that only details of the microscopic interactions need to be specified, and no assumptions are made about the character of the processes under study. The MD method has been extensively used for the analysis of the sputtering processes where desorption is a consequence of momentum transfer in the collision cascade,[23] fast nonequilibrium phase transiton,[24] or high-pressure buildup in the vicinity of the ion track.[25−28] On the other hand, there have been few MD simulations of laser ablation. The differences between ablative photodecomposition and thermal processes in organic polymers have been discussed,[18,19] and preliminary results from MD simulations of micromachining of silicon surfaces by ultrashort laser pulses have been reported recently.[29]

The factors that sufficiently increase computer time consumption and hamper the application of the MD method to the analysis of laser ablation are the relatively long laser pulse times compared to the energy deposition times for ion-induced sputtering and the sufficiently larger number of molecules (and atoms!) involved in the ablation process. Specifically, sputtering has been modeled by $\sim 10^4$ atoms for times $\approx$ 10 ps. Laser ablation has been proposed[3,5] to be a collective phenomenon involving tens of thousands of *molecules* and laser pulse widths of picoseconds to nanoseconds with concomitantly longer ejection times. This system is too large to model by brute force MD methods in terms of both the number of atoms and the time scale required.

There has been an attempt, however, to address the matrix-assisted laser desorption phenomenon by conventional atomic-level MD by Bencsura and Vertes.[20] They have clearly demonstrated both the attractive sides of the MD method and the severe restrictions on the size of the model and the time of the simulation. They explicitly include 202 matrix molecules and one analyte molecule and follow the atomic motions for 45 ps. They were able to follow the dynamics of disruption of the hydrogen bonds due to the instantaneous temperature jump representing the laser pulse. The small size of the model ($\sim$2 nm), however, could certainly have a profound impact on many aspects of the simulated phenomenon and hampers the direct

[⊗] Abstract published in *Advance ACS Abstracts,* March 1, 1997.

S1089-5647(96)03401-3 CCC: $14.00

correlation of predictions with experimental observations. Moreover, the details of the laser pulse characteristics have not been specified.

In the present work we present an approach aimed at overcoming these limitations by extending the time scale and length scale of the MD model for laser ablation. This approach makes use of the fact that molecules in organic solids have a tightly bound internal structure and form a weakly bound external structure.[30] This feature distinguishes molecular solids from other forms of matter and allows one to treat the external and internal molecular motion separately. To account for the finite rate of the vibrational relaxation of excited molecules and still be able to simulate the collective effect of laser ablation, we propose a model of breathing spheres, a model with true translational but approximate internal degrees of freedom. In this model all molecules are represented by spherical particles. The internal molecular motion is represented in a very approximate way, which, however, allows one to reproduce a realistic rate of the conversion of internal energy of the excited molecules to translational motion. This approximation permits a reasonably large number of molecules to be treated in the simulation study and, hence, leads to information about the collective effect of laser ablation. Moreover, since the vibrational motion, especially for light H atoms, is not being followed explicitly, a large time step in the numerical integration can be used.

In the following section we give a detailed description of the proposed breathing sphere model for the laser ablation of organic solids. The model is then applied to the investigation of the laser ablation of molecular films. The computational setup for the simulation of the molecular systems is given in section III. Preliminary results of the MD simulation performed on both two-dimensional (2D) and three-dimensional (3D) versions of the model are presented in section IV. The 2D simulation offers a clear visual picture of the ablation process and helps one to understand the basic ideas about the mechanisms leading to the laser ablation and the subsequent processes in the ejected plume in considerably shorter computer time. The 3D model has the advantage of directly mapping to experimental conditions in which a quantitative comparison between the computed and experimental results can be made. The summary of the work is given in section V.

II. The Model

The microscopic effect of laser irradiation falls into two broad categories: vibrational excitation and photochemical-induced fragmentation. Vibrational excitation can occur with infrared (IR) as well as with ultraviolet (UV) irradiation. In the case of IR irradiation the laser light is resonantly absorbed into OH or NH stretching vibratins.[12] With UV irradiation electronic excitations of molecular chromophores (typically a pyridine ring or another aromatic π-electron system in a matrix molecule) relax by internal conversion[11] to the vibrational excitations of a molecule. Redistribution of intramolecular energy that initially appears in particular vibrational modes of an excited molecule has been found to be fast, within ~1 ps,[31,32] and is followed by a much slower process of cooling of the vibrationally hot molecule. Computer simulations of the process of vibrational cooling give characteristic times of a few tens of picoseconds,[33] which is consistent with the observation of a 20 ps onset for the ablation process.[34] Alternatively, UV light can also photofragment the molecule. In this scenario, the laser energy is expended in breaking chemical bonds and forming molecules with smaller numbers of atoms. The resulting molecules occupy a larger volume and create pressure inside the irradiated volume,

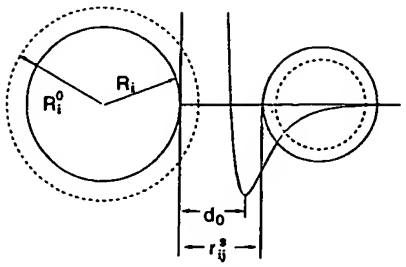

Figure 1. Potential of intermolecular interaction. R_i^0 and R_i are the equilibrium and instantaneous radii of the particle i; d_0 and r_{ij}^s are the equilibrium and instantaneous distances between the edges of the spherical particles.

which can then convert to translational energy of ablation. The process of energy transfer in this case is considerably faster than vibrational relaxation mentioned previously.[18,19] Both of the possible results of a photon absorption, photofragmentation and vibrational relaxation of an excited molecule, are incorporated in the breathing sphere model described below.

The effect of the internal excitation of matrix molecules by the laser pulse and the relaxation of the excited molecules are described by a breathing sphere model. Three translational and one internal degree of freedom are attributed to the breathing sphere representing an organic molecule. The Lagrangian, L, that describes the motion in the system of these interacting molecules is given by

$$L = 1/2\sum_i m_i(\mathrm{d}r_i/\mathrm{d}t)^2 - \sum_{ij}U_r + 1/2\sum_i M_i(\mathrm{d}R_i/\mathrm{d}t)^2 - \sum_i U_R \quad (1)$$

where m_i, r_i, and R_i are the mass, position, and radius of the ith molecule, as shown in Figure 1. The inertia or effective mass of the internal motion is denoted by M_i. The potential among the particles is U_r and the internal potential is U_R, both of which are defined below.

The interaction among the organic molecules is assumed to be pairwise additive as

$$U_r = \epsilon_n[\exp\{-2\alpha(r_{ij}^s - d_0)\} - 2\exp\{-\alpha(r_{ij}^s - d_0)\}] \quad (2)$$

where $r_{ij}^s = |r_j - r_i| - R_i - R_j$, as shown in Figure 1, with the equilibrium distance d_0 defined as the distance between the edges of the spherical particles rather than their centers. This choice of equilibrium distance is based on the physical concept that the sublimination or cohesive energy of an organic solid is governed primarily by the interaction among atoms on the outside of the molecule. This description allows an easy means of simulating a multicomponent organic solid without introduction of additional specific potentials for different types of organic molecules (i.e. matrix, analyte (big), and photofragmented (small)).

An internal degree of freedom is attributed to each molecule by allowing the spheres representing the organic molecules to change their sizes. The characteristic frequency of the internal motion is controlled by the parameters of the anharmonic potential ascribed to the internal degree of freedom:

$$U_R = k_1\Delta R_i^2 + k_2\Delta R_i^3 + k_3\Delta R_i^4 \quad (3)$$

where $\Delta R_i = R_i - R_i^0$, as shown in Figure 1. The rate of the intermode energy transfer (primarily vibrational) is determined by the size of the anharmonicity and frequency mismatch between vibrational modes.[25,35,36] Thus, the parameters of the internal potential can be used to affect the coupling between

internal molecular motion and phonon modes and to achieve a desired rate of energy transfer from an excited molecule.

The effect of laser irradiation is simulated by vibrational excitation or photofragmentation of random molecules during the time of the laser pulse within the penetration depth. The absorption probability can be modulated by Beer's law[3] to reproduce the exponential attenuation of the laser light with depth. In this case the probability for a given molecule to be excited depends on the fluence of the laser pulse and the position of the molecule under the surface relative to the penetration depth. Vibrational excitation is modeled by depositing a quantum of energy equal to the photon energy into the kinetic energy of internal vibration of a given molecule. In other words, the third term in eq 1 gets a corresponding instantaneous increase. The photofragmentation, when an excited molecule reacts photochemically and forms fragments, can be simulated within the model in two different ways. An instantaneous increase of the *equilibrium* radius of an excited molecule, R_i^0, can be used to represent an increase in the volume occupied by the reaction products.[18,19] This increase of R_i^0 shifts ΔR_i to the repulsive part of the internal potential, eq 3, and creates a local pressure pulse in the vicinity of the excited molecule. The pressure pulse can then dissipate to the thermal energy of the irradiated volume or, at high fluences, convert to the translational energy of ablation.[18,19] An alternative way of simulation of a photofragmentation event is to replace the sphere representing a molecule to be excited with several smaller spheres representing the resulting photofragmented molecules. The advantage of this approach is that the fate of the fragments can be followed during the course of the MD simulation and their role in the ablation process can be analyzed.

III. Computational Setup for the Laser Ablation of Molecular Films

The MD model described above is applied in this work to simulate laser ablation due to vibrational excitations in molecular systems. The parameters of the model chosen for this particular application are given in this section.

A. The sizes of the Model and Boundary Conditions. Two-dimensional simulations have been performed for hexagonal close-packed crystallites of sizes 81 × 210 nm (model A), 81 × 70 nm (model B), and 40 × 35 nm (model C) consisting of 58 800, 19 600, and 4950 matrix molecules, respectively. The smaller model is used primarily for pictorial renditions. For 3D simulations an amorphous molecular solid of dimensions 10 × 10 × 40 nm consisting of 27 648 matrix molecules is used. A smaller amorphous solid was first prepared from a close-packed crystal consisting of 864 molecules. Melting of the crystallite and subsequent quenching from the melt leading to the material amorphization has been simulated using the Andersen–Nose constant-pressure MD technique.[37] The 864 molecule amorphous solid is then replicated to generate the larger computational cell.

Periodic boundary conditions in the direction parallel to the surface are imposed. The bottom molecules are held rigid in the case of the 2D model. More complex boundary conditions at the bottom of the 3D model are discussed later in this section. Periodicity in the direction parallel to the surface simulates the situation in which the radius of the laser beam is large compared to the penetration depth so that the effect of the edges of a laser spot can be neglected. In other words, processes occurring in the center of the laser beam are being examined.

The boundary condition at the bottom of the computational cell can significantly influence the results of the simulations and requires special consideration. The high pressure associated with the ablation process[38,39] generates a pressure pulse that propagates into the surrounding material. The pressure pulse develops into a shock wave that gradually attenuates due to the interaction with the following unloading wave and dissipation into internal energy of material across the shock wave.[38–40] The small size of the MD computational cell does not allow a direct simulation of the attenuation process and inevitably leads to artificial border effects. Rigid boundary conditions, used in 2D simulations, lead to the reflection of the shock wave from the rigid layer and a temporal spike of the compressive pressure in the border region. The reflected shock wave then reaches the surfae and can contribute to the material ejection.[25,27]

In the case of the 2D model, however, we can afford to deal with the problem of the bottom boundary condition by merely increasing of the size of the computational cell. The velocity of propagation of the pressure wave in the 2D model of an organic solid is calculated to be 2760 m/s, and for models A and B it takes respectively about 120 and 40 ps for a pressure wave to cover the distance between the high-pressure region formed within the penetration depth and the rigid layer, to be reflected, and to reach the surface. The processes of the matrix disintegration and ejection are rapid and occur prior to the time in which the surface region is subjected to the reflected shock wave even for the smaller model B. Thus the effects of the ablation and the surface response to the reflected pressure wave are separated in time and can be analyzed independently. Additional testing of the effect of the boundary condition is performed by comparing the results for model B with results for the bigger model A where the surface region does not feel the boundary effects up to 120 ps after the ablation initiation.

In the case of the 3D model we are using a different approach because a further increase of the computational cell is too computationally expensive. In this case we follow the recipes for the reduction of the effects of the reflected shock wave proposed in the MD simulations of sputtering.[24,26,28] In particular, we increase the mass of the molecules in the bottom 8 Å by a factor of 10 and apply the velocity dampening technique, where the velocity of every molecule within the bottom 40 Å is taken to be zero every time the kinetic energy of the molecule maximizes. This condition allows us to minimize the effect of the shock wave reflection and to avoid shock-induced fracturing of the matrix for laser fluences reported in this paper. Prescriptions for accurately damping the shock wave are under investigation.

B. The Potential Parametrization and the Laser Energy Deposition. For the simulations presented in this paper a set of parameters ($d_0 = 3$ Å, $\epsilon_n = 0.1$ eV, $\alpha = 1$ Å^{-1}) have been chosen. For matrix molecules with a mass of 100 Da and an equilibrium radius R_i^0 of 1.4 Å (Figure 1), the predicted properties of a 3D molecular solid are as follows: sublimination energy of 0.6 eV, elastic bulk modulus of ~5 GPa, density of 1.2 g/cm^{-3}, and phonon spectra with a single broad band centered at 45 cm^{-1} with a width of ~50 cm^{-1}, as shown in Figure 2. These values are typical for molecular solids.[30]

As mentioned above, the proposed breathing sphere model allows one to easily incorporate other species. In the present work analyte molecules with a mass 20 times that of the matrix molecules and $R_i^0 = 10$ Å are introduced into the 2D model. Each analyte molecule replaces in this case 18 matrix molecules. The positions for eight (model C) or 30 (model B) analyte molecules to be introduced are chosen at random, and the results for five runs with different initial configurations are averaged for model B in order to obtain statistically significant data on the ejection of analyte molecules.

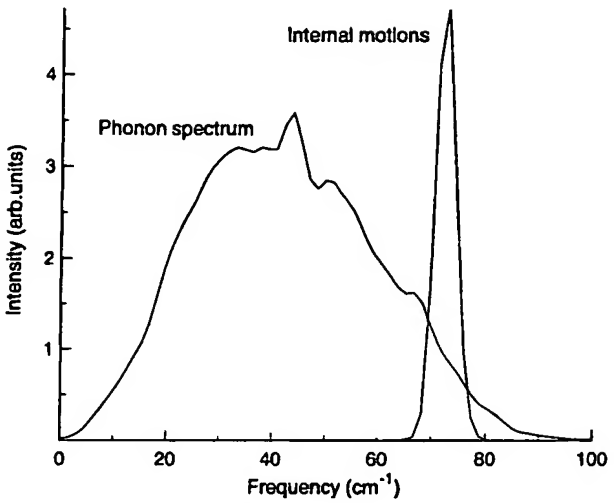

Figure 2. Vibrational spectrum of the 3D model of organic solid calculated at 300 K. Internal molecular motion is represented by one vibrational mode.

For the calculations presented in this paper the parameters of the internal potential ($k_1 = 30$ eV/Å^2, $k_2 = -60$ eV/Å^3, $k_3 = 60$ eV/Å^4, and the inertia parameter M equal to 5000 and 3200 Da in 2D and 3D simulations, respectively) are chosen to provide the characteristic time of the cooling of an excited molecule to be on the order of 10 ps.[33] The spectral peak corresponding to the internal vibrations in this case is embedded into the high-frequency tail of the phonon spectrum as shown in Figure 2 for the 3D system.

The laser irradiation in the present work is simulated by vibrational excitation of random matrix molecules. The total number of photons entering the model solid during the laser pulse is determined from the laser power and the pulse width. In the 2D model the absorption probability is evenly distributed over a penetration depth of 32 nm. The results of the 3D simulation are used for qualitative comparisons with experimental data, and the exponential decrease of the absorption probability with depth is simulated in accordance with Beer's law. A penetration depth of 7 nm is used in this case in order to provide an absorption of 99% of the laser energy within the computational cell. Laser pulses of 15 ps in duration at a wavelength of 337 nm (3.68 eV) are used in the simulations. The photon energy is scaled down by a factor of 2 for the 2D model in order to account for the lower cohesive energy of molecules in the 2D crystallite as compared to the 3D case. Note that in the case of UV irradiation an excited molecule can break up and form fragments. The role of photofragmentation under conditions typical for UV-MALDI experiments is not firmly established, but it is typically believed not to be dominant.[11] Thus, while the model allows us to account for photofragmentation processes, as discussed in section II, this has not been done in the present work. The characterization of the ablation process driven by the photofragmentation of excited molecules is a subject of our current study.

C. Analysis of Simulation Results. The MD simulation technique allows one to perform a detailed analysis of the laser ablation processes in which macroscopic parameters of the system can be correlated with data on microscopic dynamics at the molecular level. Velocity, angle, and ablated cluster distributions can be calculated for both matrix and analyte molecules. These characteristics are closely related with the quality of the mass spectra and can be directly compared with experimental observations. At the same time a number of local physical characteristics are used to describe the system at the molecular level. The energies and velocities of molecules are obtained directly from the MD algorithm. The Dirichlet construction[41] has been used to define the volume per molecule or local density and the coordination number of each molecule in the 2D model. The coordination numbers are conventionally used for characterization of the defect structure of 2D systems.[41-43] All varieties of structural defects in 2D crystals can be identified in terms of groups of non-6-fold coordinated particles,[41,42] and the melting corresponds to the rapid increase of the defect density.[41,43] Thus, calculation of the number of non-6-fold coordinated molecules can provide a quantitative description for the structural changes and phase transitions occurring in the 2D model. To calculate pressure at the location of a molecule, the concept of local atomic stresses commonly used in computational material science[44] has been extended for these molecular interactions, and the local hydrodynamic pressure is defined as a first invariant of the stress tensor. The vibrational spectra (Figure 2) are computed by taking the Fourier transform of the velocity−velocity autocorrelation functions.[36]

A Nordsieck predictor−corrector algorithm is used to integrate the equations of motion.[45] The largest simulation performed here is ~60 000 molecules for 1 ns at a time step of 5 fs. This simulation required ~1 CPU hour on an IBM RISC 6000 computer for each 1 ps of molecular motion. A typical matrix molecule (e.g. cinnamic acid) has 19 atoms. To follow H atom vibrational motion, a time step of ~0.1 fs must be used. If explicit atoms were included in this simulation, the computer time would increase by a factor of ~10^3. Since each simulation for the breathing spheres already takes several days, including explicit atoms would be computationally prohibitive.

IV. Results and Discussion

In this section we present the results of the MD simulation of the laser ablation of molecular systems. These results demonstrate the capabilities of the breathing sphere model and provide insight into the fundamental processes involved in the ablation phenomenon. First, based on the results of the 2D simulation, a qualitative analysis of the processes and mechanisms leading to the matrix disintegration and collective ejection is presented. The processes in the ejected plume and the ejection parameters of big analyte molecules incorporated into a matrix are then discussed. Finally, preliminary results obtained for the 3D model are used to support the conclusions based on the 2D simulation and to make direct comparisons with experimental results.

We start with a discussion of the results of the 2D simulation for laser irradiation of 15 ps pulse duration. For this discussion we have chosen a fluence that leads to ablation. A total of 16% of the molecules were each given 1.84 eV of kinetic energy in the internal mode. This corresponds to a total energy density of 0.30 eV deposited per matrix molecule within the penetration depth. This deposited energy density is slightly less than the cohesive energy of 0.31 eV of the 2D model organic solid. Three snapshots of the simulation are shown in Figure 3 for model C (4806 matrix and eight analyte molecules). Qualitatively the picture fits with the conventional wisdom of laser ablation. Most but not all of the molecules in the irradiated region are being ablated and the analyte molecules are moving at about the same velocity as the matrix molecules (or conversely, the analyte molecules are not getting left behind). The structure of the ejected plume and the results concerning the analyte molecules will be discussed later in this section. First we shall perform a detailed analysis of the processes in the irradiated material leading to ablation.

The spatial and time development of the internal or vibrational energy of molecules, the local hydrostatic pressure, and the

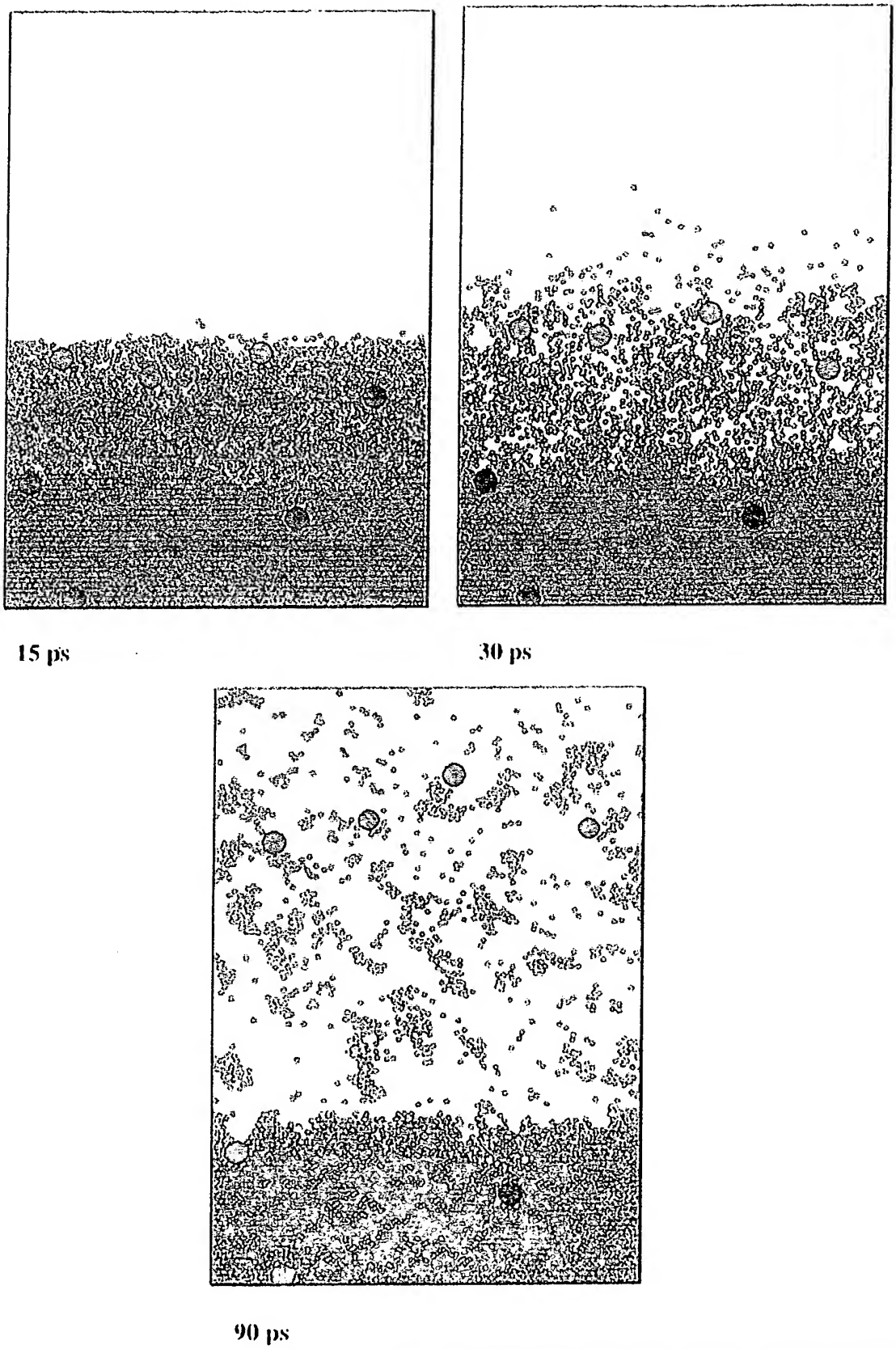

Figure 3. Snapshots from a MD simulation of laser ablation, model C. The blue and red small spheres represent unexcited and excited matrix molecules. The larger green spheres represent analyte molecules.

defect density in the material are presented for model A (58 800 molecules) in the form of contour plots in Figure 4. The model sample is divided into 105 horizontal zones, and contour plots are drawn through the points corresponding to the average of the quantity for all the molecules in the zone. In the case of model A, one zone consists of 560 molecules or four molecular monolayers. In other words, each data point corresponds to the averaging over 560 molecules that are *initially* situated at

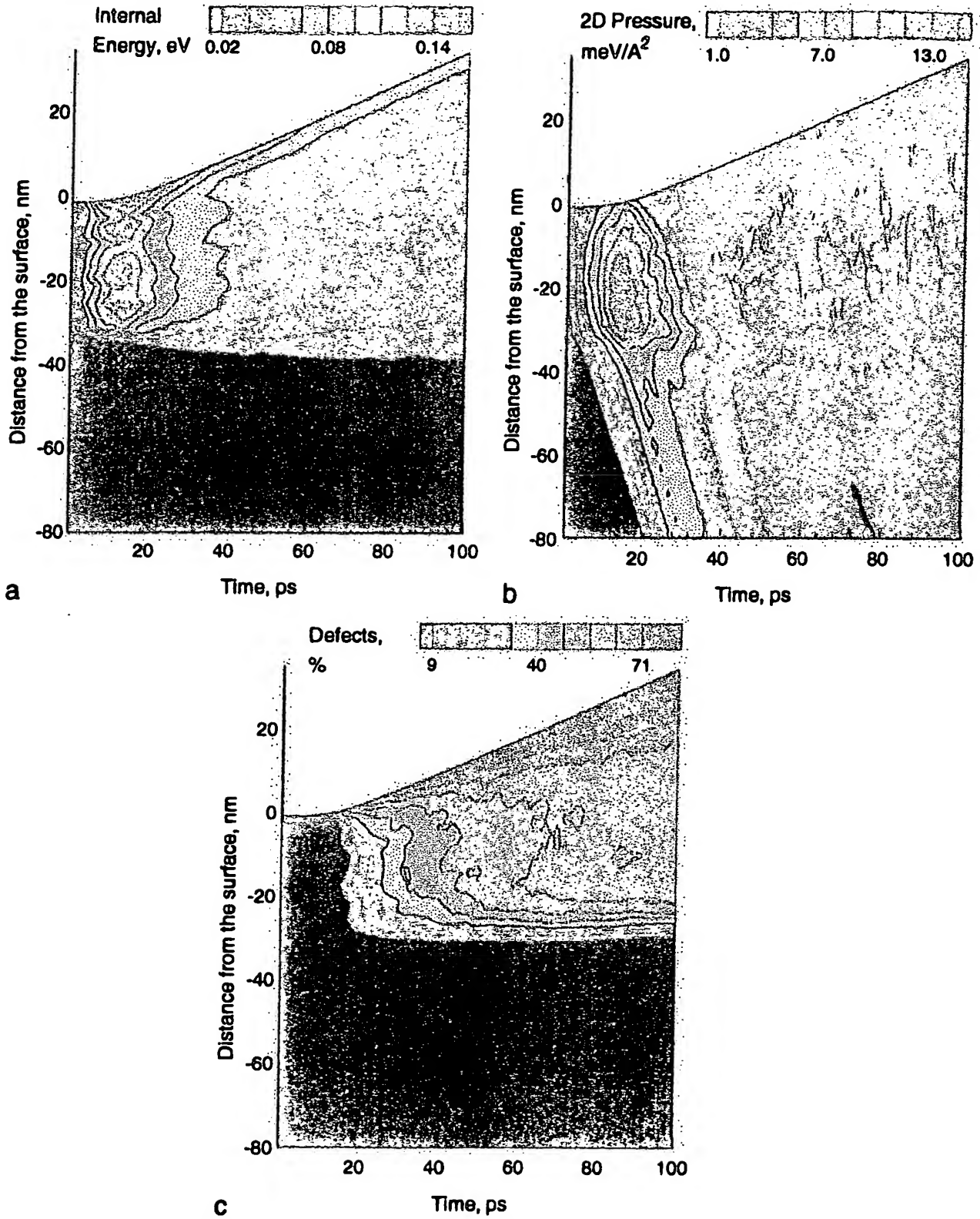

Figure 4. Spatial and time distributions for model A: (a) internal molecular energy; (b) local hydrostatic 2D pressure; (c) defect density. The laser pulse is 15 ps and the penetration depth is 32 nm. The depth shown is 80 nm and the entire sample is 210 nm.

nearly the same depth in the sample. The data points are calculated at 1 ps intervals during the MD trajectories starting from the beginning of a laser pulse. The data for the upper 80 nm of the sample (40 zones) for the first 100 ps of simulation are presented in Figure 4. The abscissa is the average vertical position of each zone; thus the nonrectangular shape of the contour plots reflects the ejection of part of the irradiated volume. The material characteristics averaged over the upper 24 nm (12 zones) are plotted in Figure 5.

Figure 4a shows that the internal energy of molecules within the laser penetration depth increases during the pulse duration due to the laser light absorption. The internal energy then

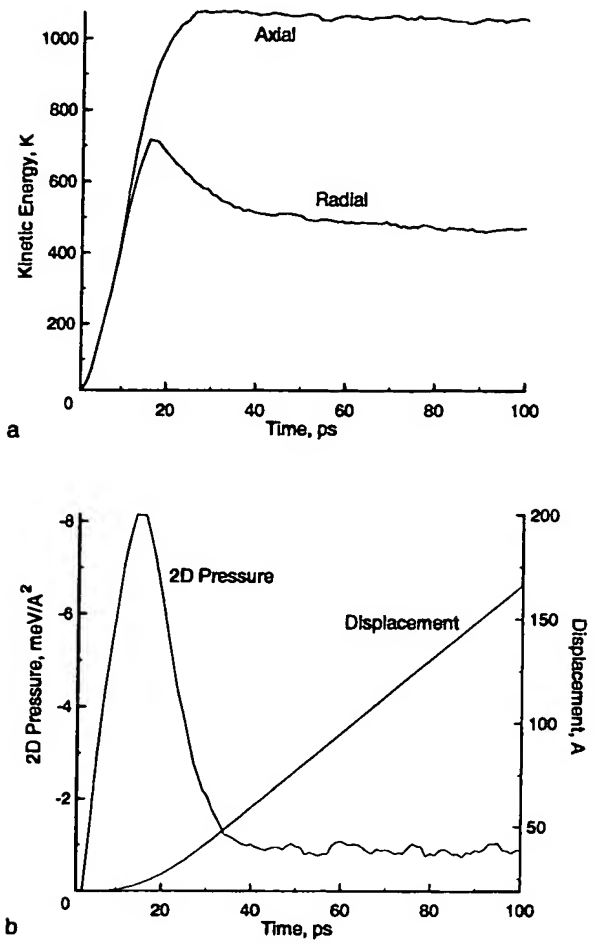

Figure 5. Material characteristics versus time. All quantities are averaged over the molecules in the original top 24 nm of the system. The results are for the 2D simulation shown in Figure 1a. (a) Axial and radial kinetic energies. The kinetic energies are given in Kelvin, but no implications about equilibrium are made. (b) 2D pressure and displacement.

equilibrates with the thermal energy of translational motion of molecules within 10−20 ps. The energy transfer in molecules from the top layers is slower due to fewer intermolecular interactions and ejection of excited molecules that have insufficient time to relax.

The rapid energy transfer from the vibrationally excited molecules results in intensive energy pumping into the thermal energy of the organic crystal and a sharp temperature rise within the laser penetration depth on the time scale of the pulse duration, Figure 5a. The heating rate of the material is faster than the material can undergo thermal expansion, and a high pressure builds up in the irradiated volume, Figures 4b and 5b. This high pressure formed within the penetration depth then relaxes by expansion of the irradiated material. In the direction down from the surface, the relaxation of the laser-induced pressure drives a strong compression wave into the cold part of the sample, Figure 4b. In the opposite direction, the pressure gradient leads to the forces driving the acceleration of the top layers in the direction normal to the surface. That can be seen from Figure 5b, where the average displacement of the upper 24 nm (the biggest part of irradiated volume) is plotted. The acceleration of the region as a whole starts at ~10 ps, when the pressure reaches a high level, and is over at ~25 ps, when the pressure drops down. The displacement then increases linearly with time, indicating that the whole region is ablated and moves away from the sample with an *average* velocity of 200 m/s. We find that the velocities of the ejected particles are nonuniformly distributed in the plume, and the momentum transfer from the lower particles to the top particles results in the high, ~700 m/s, plume-front velocities in the 2D model.

Additional insight into the picture given above of ablation driven by the dynamics of the pressure relaxation comes from examining the thermodynamic and structural characteristics of the ejection process. The melting temperature of the 2D system is found to be about 400 K when melting is simulated by slow heating at zero pressure. The rapid heating of the material exposed to a short laser pulse causes strong compressive pressures, which can suppress the initiation of the melting phase transition up to a high degree of overheating. To have a quantitative description of the structural and phase changes in the model, we monitor development of the defect density distribution, Figure 4c. Except for the shallow surface region, no defects are detected during the most of the 15 ps laser pulse. Only close to the end of the laser pulse, when the average kinetic energy within the penetration depth reaches ~700 K, Figure 5a, does the defect density start to rise sharply and nearly linearly with time, Figure 4c. During the short time span between 15 and 30 ps the defect density is increasing up to the level that far exceeds the one characteristic of the liquid state. It is noteworthy that this increase starts simultaneously and proceeds with nearly the same rate in the whole irradiate part of the sample. This points to a rapid *homogeneous* phase transition/explosion from a solid directly to a gaseous phase consisting of a mixture of sublimated molecules and molecular clusters. On the basis of thermodynamic considerations, the phase explosion or homogeneous explosive boiling has been indeed predicted to occur under conditions of intensive laser irradiation.[46,47] A more detailed analysis of the nature of the nonequilibrium phase explosion and its connection to the threshold behavior in laser ablation will be given elsewhere.[48]

The phase explosion contributes to buildup of the high pressure in the material despite the quick expansion. In this regard the phase explosion plays the same part as thermochemical processes in the picosecond laser ablation of polymers.[49] Another important consequence of the phase explosion is the fast cooling of the ejected plume due to the adiabatic expansion and intensive disintegration of the matrix.[50] The kinetic energy of thermal motion is tranferred into the potential energy of material disintegration and the flow energy of the ejected plume. The time dependence of the average kinetic energy of molecular motion parallel (radial) and perpendicular (axial) to the surface is shown in Figure 5a. The divergence of the axial and radial kinetic energies starts at 10 ps coincidentally with the laser pressure induced expansion and acceleration, Figure 5b, of irradiated volume. This acceleration is responsible for the sharp increase of the axial kinetic energy, which nearly doubles during the short period of pressure relaxation (10−25 ps). The energy of the material flow out of the surface accounts for the biggest part of this increase of axial kinetic energy. At the same time, the cooling of the expanding material starts to compete with the laser energy pumping into the thermal energy and reduces the rate of the increase of the radial kinetic energy, Figure 5a. The radial kinetic energy then decreases quickly, within 15 ps, Figure 5a. This decrease coincides in time with the phase explosion, Figure 4c, indicating that the cooling is the result of the explosive matrix disintegration. This cooling affects equally the radial and axial kinetic energies. In the case of the axial kinetic energy the cooling competes with the concurrent axial acceleration of the ejected material and is not apparent in Figure 5a. In MALDI, the fast cooling of the ejected plume due to the phase explosion and the short time that analyte molecules

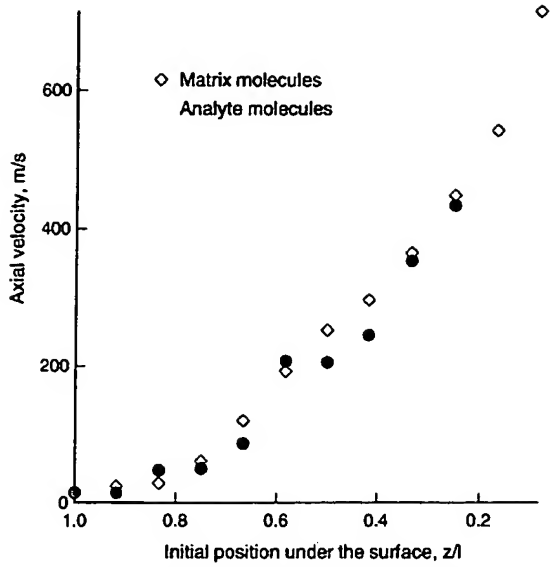

Figure 6. Axial velocities of matrix and analyte molecules at a time of 500 ps as a function of their initial position under the surface, z, relative to the laser penetration depth, l. The data points correspond to the averaging of the results of five runs for model B.

remain in the energetic environment created by the laser pulse are the conditions that can preserve the analyte molecules intact.[16]

The phase explosion of a metastable overheated liquid results in the ejection of the plume consisting of the molecular clusters or liquid droplets of different sizes along with the individual molecules. The velocities of the ejected clusters and molecules are nonuniformly distributed in the ejected plume. The molecules that originate from the top layers acquire higher axial velocities at early times, ~10−20 ps, after the laser impact. We find that intermolecular collisions in the plume lead to additional changes in the axial energy profile. The axial velocity of the molecules from upper layers continues to increase even after they are ejected high above the surface. This energy and momentum transfer from the lower layers to the top layers results in the high maximum velocities of the plume expansion, Figure 6, and strongly forwarded ejection as observed in MALDI experiments.[6-8,13] As a result of the collective ejection process, the big analyte molecules get axial acceleration from an expanding plume and move along with the matrix molecules at approximately the same velocity, Figure 6. There is a difference in the statistical significance of the points in Figure 6 for matrix and analyte molecules, where each point corresponds to the average velocity of either ~3000 matrix molecules or four to seven analyte molecules.

In contrast to the axial velocities, we find that the radial velocities of the ejected molecules have no significant correlation with the initial position of molecules under the surface. The fast decrease in the radial kinetic energy due to the explosive matrix disintegration discussed above is followed by a much slower gradual cooling of the ejected material down to the melting point. This process has been connected with the cluster decomposition. We find that both processes of the axial energy redistribution and the radial cooling in the plume last longer than the time of our simulation, 1 ns. A more detailed analysis of the processes in the plume and their role in the formation of the final velocities and angle distributions will be given elsewhere.[51]

The preliminary results of the simulation performed on the 3D model agree well with the qualitative scenario for the ablation process outlined above on the basis of the 2D results.

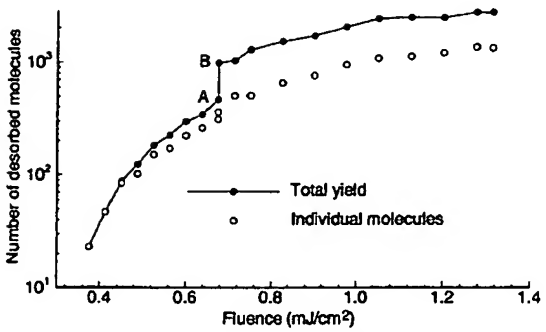

Figure 7. Ablation yield as a function of laser fluence for the 3D model of the molecular solid.

To reproduce a yield−fluence relationship for the 3D model and determine the threshold fluence for the ablation, we have performed a series of simulations at different laser fluences. We find that at a laser fluence of 0.4 mJ/cm^2 a noticeable number of molecules start to desorb from the surface, Figure 7. The yield gradually increases to a fluence of 0.675 mJ/cm^2, point A in Figure 7, where a stepwise increase of the total yield occurs. We have repeated the simulation at 0.675 mJ/cm^2 four times and obtained a total yield of ~500 molecules three times and about 1000 molecules once, points A and B in Figure 7, respectively. Increasing the irradiation dose beyond 0.675 mJ/cm^2 leads to the monotonic increase of the yield with clear evidence of saturation at high fluences. Both the sharp initial increase of the molecular yield and the saturation at high fluences are features typical of experimental results.[5,9,10,14]

The most prominent feature of the calculated curve is the stepwise increase in the total yield at 0.675 mJ/cm^2. This feature clearly breaks the ejection process into two distinct regions. We find that there is a dramatic difference in the plume structure that corresponds to the low- and high-fluence portions of the curve in Figure 7. Primarily single molecules with a small number of molecular dimers and trimers are ejected at fluences lower than 0.675 mJ/cm^2. This indicates that the ejection mechanism at these fluences is an intensive surface vaporization. Starting from point B the ejected plume is found to contain a substantial fraction of large molecular clusters. In particular, the fraction of ejected molecules in clusters composed of 10 or more molecules increases from 2% of the total yield for point A up to 41% for point B and then gradually decreases down to ~20% at highest fluences simulated. This clearly indicates that the mechanism of ejection changes at the fluence of 0.675 mJ/cm^2 from evaporation to the collective ejection process or ablation. Preliminary analysis indicates that the physical picture of the ablation process presented above for the 2D model is valid also for the 3D system.

Comparing the simulation data with experimental mass spectrometry measurements,[3-14] one should take into account the difference between the total yield and the yield of individual particles that are shown in Figure 7. The commonly measured fluence dependence of the yield of individual particles is found to have no step increase at the ablation threshold. This suggests that the experimental threshold for matrix molecules corresponds to a detection threshold[9] in the evaporation regime, whereas the ablation threshold predicted by the model is likely to correspond to the real physical threshold for the ejection of large analyte molecules in MALDI.[5] In this case the observation of Ens et al.[5] that at the threshold fluence either a large number of analyte ions are produced in a *successful* event or none at all can be directly correlated with the existence of *certain probability* for the triggering of the ablation at the threshold in our model.

For quantitative comparisons between the computed and experimental threshold fluences we take into account the fact that the penetration depth used in the 3D model is underestimated by a factor of ~20 compared to the typical UV-MALDI conditions.[3] Thus about 20 times higher fluence would be required to produce a similar distribution of the deposited energy within a realistic penetration depth. This rough estimation gives us an ablation threshold of ~10−20 mJ/cm^2 that reasonably matches the experimental values.[3,5,9,10] We should point out, however, that exact quantitative scale up of the simulation results to experimental conditions is impossible. Different processes that determine the desorption and ablation phenomenon have different dependences on the laser penetration depth and pulse duration. The development of the nonreflecting boundary conditions and parallelization of the MD code should allow us to additionally extend the time and length scales of the model and perform a more justified extrapolation to the typical experimental conditions.

Finally we note that the 3D model predicts higher maximum velocities of the ejected molecules than the ones predicted by the 2D model, Figure 6. The average velocity of the molecules originated from the top layer (that would correspond to the rightmost point in Figure 6 in the case of the 2D model) is found to vary between 600 m/s at the ablation threshold up to 1500 m/s at the highest simulated fluence of 1.3 mJ/cm^2. This result is in good agreement with the reported velocities of the plume expansion.[6−8,13,14]

V. Summary

The relatively long time scale and large number of molecules involved in laser ablation are the factors that have hampered the application of molecular dynamics simulations in this field. To overcome these limitations, we propose a MD model of breathing spheres, a model with true translational and approximate internal degrees of freedom. The main features of the proposed model are as follows:

(i) Experimental parameters such as laser power and wavelength, pulse width, and penetration depth are used to simulate the laser irradiation.

(ii) Microscopic effects of molecular excitation by photon absorption (photochemical reactions, vibrational excitations) are included, and the issue of thermal versus photochemical ablation can be addressed.

(iii) An internal degree of freedom is introduced to reproduce a realistic rate of vibrational relaxation of the excited molecules.

(iv) An approximate representation of the internal molecular motion permits a significant increase in the number of molecules to be treated in the simulation study. Up to 58 800 molecules are included in a computational cell used in the present work.

(v) Several types of molecules can be incorporated into the model to simulate complex organic solids.

(vi) Development of temperature, pressure, and energy distributions in the system can be calculated and compared with experimental data and predictions of analytic models.

The model is applied in this work to the investigation of the laser ablation of molecular systems. The 2D and 3D models are used in concert to sort out the important phenomena and correlate them to experimental conditions and observations. We believe that the model provides a realistic description of the ablation process. In particular, the calculated yields versus fluence dependence has a stepwise increase of molecular yield with increasing fluence and saturation at high fluences. A well-defined threshold fluence has been found to separate two distinct mechanisms for the ejection of molecules, surface vaporization at low laser fluences and collective ejection or ablation at high fluences. A stepwise increase of the yield and a fundamental change in the structure of the ejected plume are predicted to occur at the threshold fluence. Above the threshold the laser-induced high pressure and the explosive homogeneous phase transition from a solid directly to a gaseous phase consisting of mixture of sublimated molecules and molecular clusters lead to the strongly forwarded emission of ablated material and high, from 500 up to 1500 m/s, maximum velocities of the ejected plume expansion. Large molecular clusters are found to constitute a significant part of the ejected plume at fluences close to the ablation threshold.

The model predicts that the processes in the plume significantly influence the final velocities and angle distributions. Intermolecular collisions in the plume lead to the axial energy and momentum transfer from the lower layers to the top layers. This effect can significantly contribute to the high maximum velocity of the plume expansion and large velocity spread observed for matrix molecules in MALDI experiments. At the same time the radial kinetic energy of the ejected molecules is found to have no significant correlation with the initial position of molecules under the surface. The explosive phase transition and matrix disintegration cause a fast decrease in the radial energy. Subsequent plume expansion and cluster decomposition lead to the additional gradual radial cooling of the ejected material.

Large analyte molecules incorporated in the matrix get axial acceleration from an expanding plume and move along with the matrix molecules at nearly the same velocity. The fast cooling of the expanding plume can be an important factor that provides the conditions for the large analyte molecules to survive volatilization.

Acknowledgment. We gratefully acknowledge financial support from the Office of Naval Research through the Medical Free Electron Laser Program and the National Science Foundation. The computational support for this work was provided by the IBM-Selected University Research Program and the Center for Academic Computing at Penn State University. We appreciate helpful discussions with R. Srinivasan, R. F. Haglund, D. Dlott, R. J. Levis, and F. Hillenkamp.

References and Notes

(1) *Proceedings of Laser−Tissue Interaction VII*; Jacques, S. L., Ed.; SPIE Proceedings Series 2681; 1996.

(2) *Methods and Mechanisms of Producing Ions from Large Molecules*; Standing, K. G., Ens, W., Eds.; NATO ASI Series 269; Plenum Press: New York, 1991.

(3) Karas, M. In *Fundamental Processes in Sputtering of Atoms and Molecules (SPUT 92)*; Sigmund, P., Ed.; Det Kongelige Danske Videnskabernes Selskab: Copenhagen, 1993; p 623.

(4) Karas, M. *Biochem. Mass Spectrom.* **1996**, *24*, 897.

(5) Ens, W.; Mao, Y.; Mayer, F.; Standing, K. G. *Rapid Commun. Mass Spectrom.* **1991**, *5*, 117.

(6) Zhou, J.; Ens, W.; Standing, K. G.; Verentchikov, A. *Rapid Commun. Mass Spectrom.* **1992**, *6*, 671.

(7) Beavis, R. C.; Chait, B. T. *Chem. Phys. Lett.* **1991**, *181*, 479.

(8) Pan, Y.; Cotter, R. C. *Org. Mass Spectrom.* **1992**, *27*, 3.

(9) Dreisewerd, K.; Schürenberg, M.; Karas, M.; Hillenkamp, F. *Int. J. Mass Spectrom. Ion Processes* **1995**, *141*, 127.

(10) Dreisewerd, K.; Schürenberg, M.; Karas, M.; Hillenkamp, F. *Int. J. Mass Spectrom. Ion Processes* **1996**, *154*, 171.

(11) Ehring, H.; Sundqvist, B. U. R. *Appl. Surf. Sci.* **1996**, *96−98*, 577.

(12) Berkenkamp, S.; Karas, M.; Hillenkamp, F. *Proc. Natl. Acad. Sci. U.S.A.* **1996**, *93*, 7003.

(13) Preisler, J.; Yeung, E. S. *Appl. Spectrosc.* **1995**, *49*, 1826.

(14) Braun, R.; Hess, P. *J. Chem. Phys.* **1993**, *99*, 8330.

(15) Johnson, R. E. In *Large Ions: Their Vaporization, Detection and Structural Analysis*; Baer, T., Ng. C. Y., Powis, I., Eds.; John Wiley: New York, 1996; p 49.

(16) Vertes, A. In ref 2; p 275.

(17) Vertes, A.; Lavine, R. D. *Chem. Phys. Lett.* **1990**, *171*, 284.

(18) Garrison, B. J.; Srinivasan, R. *J. Appl. Phys.* **1985**, *57*, 2909.

(19) Garrison, B. J.; Srinivasan, R. *Appl. Phys. Lett.* **1984**, *44*, 849.
(20) Bencsura, A.; Vertes, A. *Chem. Phys. Lett.* **1995**, *247*, 142.
(21) Venugopalan, V. In *Proceedings of Laser–Tissue Interaction IV*; Jacques, S. L., Ed.; SPIE Proceedings Series 2391; 1995; p 184.
(22) Itzkan, I.; Albagli, D.; Dark, M. L.; Perelman, L. T.; von Rosenberg, C.; Feld, M. S. *Proc. Natl. Acad. Sci. U.S.A.* **1995**, *92*, 1960.
(23) Bernardo, D. N.; Bhatia, R.; Garrison, G. J. *Comput. Phys. Commun.* **1994**, *80*, 259.
(24) Shiea, J.; Sunner, J. In ref 2; p 147.
(25) Banerjee, S.; Johnson, R. E.; Cui, S.-T.; Cummings, P. T. *Phys. Rev.* **1991**, *B43*, 12707.
(26) Urbassek, H. M.; Kafemann, H.; Johnson, R. E. *Phys. Rev.* **1994**, *B49*, 786.
(27) Fenyö, D.; Johnson, R. E. *Phys. Rev.* **1992**, *B46*, 5090.
(28) Urbassek, H. M.; Waldeer, K. T. *Phys. Rev. Lett.* **1991**, *67*, 105.
(29) Herrmann, R. F. W.; Gerlach, J.; Campbell, E. E. B. *Nucl. Instrum. Meth. Phys. Res. B*, in press.
(30) Kitaigorodsky, A. I. *Molecular Crystals and Molecules*; Academic Press: New York, 1993.
(31) Wyatt, R. E.; Iung, C.; Leforestier, C. *Acc. Chem. Res.* **1995**, *28*, 423.
(32) Kodali, P. B. S.; Garrison, B. J. *J. Chem. Phys.*, submitted.
(33) Chang, T.-C.; Dlott, D. *J. Chem. Phys.* **1989**, *90*, 3590.
(34) Kim, H.; Postlewaite, J. C.; Zyung, T.; Dlott, D. *Appl. Phys. Lett.* **1989**, *54*, 2274.
(35) Zare, R. N.; Levine, R. D. *Chem. Phys. Lett.* **1987**, *136*, 593.
(36) Zhigilei, L. V.; Srivastava, D.; Garrison, B. J. *Surf. Sci.*, in press.
(37) Likhachev, V. A.; Mikhailin, A. I.; Zhigilei, L. V. *Philos. Mag. A* **1994**, *69*, 421.
(38) Gilath, I. In *High-Pressure Shock Compression of Solids II. Dynamic Fracture and Fragmentation*; Davison, L., Grady, D. E., Shahinpoor, M., Eds.; Springer-Verlag: New York, 1996; p 90.
(39) Trucano, T.; McGlaun, J. M.; Farnsworth, A. In *Proceedings of Laser–Tissue Interaction V*; Jacques, S. L., Ed.; SPIE Proceedings Series 2134A; 1994; p 179.
(40) Boslough, M. P.; Assay, J. R. In *High-Pressure Shock Compression of Solids*; Asay, J. R., Shahinpoor, M., Eds.; Springer-Verlag: New York, 1993; p 7.
(41) McTague, J. P.; Frenkel, D.; Allen, M. P. In *Ordering in Two Dimensions*; Sinha, S. K., Ed.; North-Holland: Amsterdam, 1980; p 147.
(42) Fisher, D. S.; Halperin, B. I.; Morf, R. *Phys. Rev. B* **1979**, *20*, 4692.
(43) Nelson, D. R. *Phys. Rev. B* **1983**, *28*, 5515.
(44) Vitek, V.; Egami, T. *Phys. Status Solidi B* **1987**, *144*, 145.
(45) Nordsieck, A. *Math. Comput.* **1962**, *16*, 22.
(46) Martynyuk, M. M. *Sov. Phys. Tech. Phys.* **1976**, *21*, 430.
(47) Kelly, R.; Miotello, A. *Appl. Surf. Sci.* **1996**, *96–98*, 205.
(48) Zhigilei, L. V.; Kodali, P. B. S.; Garrison, B. J. *Phys. Rev. Lett.*, submitted.
(49) Hare, D. E.; Franken, J.; Dlott, D. D. *J. Appl. Phys.* **1995**, *77*, 5950.
(50) Sunner, J.; Ikonomou, M. G.; Kebarle, P. *Int. J. Mass Spectruom. Ion Processes* **1988**, *82*, 221.
(51) Zhigilei, L. V.; Garrison, B. J. In preparation.

Technical Proceedings 1999 International Conference on Modeling and Simulation of Microsystems (MSM '99), Applied Computational Research Society, 1999.

Mesoscopic Breathing Sphere Model for Computer Simulation of Laser Ablation and Damage

Leonid V. Zhigilei and Barbara J. Garrison

152 Davey Lab., Department of Chemistry, Penn State University, University Park, PA 16802
E-mails: leo@chem.psu.edu and bjg@chem.psu.edu

ABSTRACT

A breathing sphere model has been developed for molecular dynamics simulations of laser ablation of organic solids. The novel feature of this model is an approximate representation of the internal molecular motion, which permits a significant expansion of the time and length scales of the model, and yet still allows one to reproduce a realistic rate of the vibrational relaxation of excited molecules. A dynamic boundary condition that accounts for the laser induced pressure wave as well as the direct laser energy deposition in the boundary region allows one to focus the computational effort to the region where active processes of laser ablation and damage occur. The model has been applied to study the mechanisms of laser ablation of molecular solids, velocity distributions of ejected molecules, and laser damage in the case of spatially localized absorbers. The results for different laser fluences and pulse durations have been analyzed and related to available experimental data.

Keywords: molecular dynamics simulation, laser ablation, mesoscopic model, pressure waves, non-reflecting boundary condition.

INTRODUCTION

The interaction of laser pulses with organic matter leading to massive material removal (ablation) from a target is a subject of scientific as well as applied interest [1,2]. Important practical applications include laser surgery [3], matrix-assisted laser desorption/ionization (MALDI) of biomolecules for mass - spectrometric investigations [1,2,4] and surface microfabrication of polymer thin films [1,2].

Laser ablation of organic solids is a complex collective phenomenon that includes processes occurring at different length and time scales. The processes involved in laser ablation include laser excitation of absorbing molecules, energy transfer from the excited molecules into the internal and translational modes of other molecules in the solid, formation of a highly energetic high-temperature and high-pressure region, explosive disintegration and prompt forward ejection of a volume of material, intensive processes in the ejected plume, and propagation of the pressure wave away from the ablation region. The complex character of the involved intertwined processes hinders an adequate analytical formulation for a continuum description of the phenomenon whereas a collective character of the laser ablation occurring at the mesoscopic rather than molecular scale does not permit a direct application of the atomistic simulation approach.

An alternative mesoscopic model has been developed recently for molecular dynamics (MD) simulation of laser ablation and damage of organic solids [5,6]. The model has advantage of both addressing the effects of laser irradiation at a submicron resolution and yet incorporating a realistic description of energy relaxation of individual molecules internally excited by photon absorption.

The laser induced buildup of a high pressure within the absorbing volume and generation of the pressure waves propagating from the absorption region poses an additional challenge for molecular-level simulation. A new dynamic boundary condition is developed to account for the laser induced pressure wave propagation through the boundary of the computational cell as well as for the direct laser energy deposition in the boundary region [7].

In this paper we give a brief description of the breathing sphere model and the dynamic boundary conditions. This is followed by a discussion of application of the model to the analysis of the basic physical mechanisms of laser ablation of molecular solids. The existence of two distinct regimes of molecular ejection and the fluence dependence of the monomer yield measured in mass specrtometry experiments are addressed.

THE BREATHING SPHERE MODEL

The model assumes that each molecule (or appropriate group of atoms) can be represented by a single particle that has the true translational degrees of freedom but an approximate internal degree of freedom [5,6]. The internal degree of freedom is attributed to each molecule by allowing the particles to change their sizes. The characteristic frequency of the internal motion is controlled by the parameters of an anharmonic potential. The rate of the intermode energy transfer is determined by the size of the anharmonicity and frequency mismatch between vibrational modes. Thus, the parameters of the internal potential can be used to affect the coupling between internal and translational molecular motions and to achieve a desired rate of the conversion of internal energy of the molecules excited by the laser to the translational and internal motion of the other molecules. The rate of the vibrational relaxation of excited molecules is an input parameter in the model and can be either estimated from experimental data or modeled with atomistic or *ab initio* molecular dynamics simulations [8,9].

Technical Proceedings 1999 International Conference on Modeling and Simulation of Microsystems (MSM'99), Applied Computational Research Society, 1999.

Because the molecules and not the atoms are the particles of interest, the system size can be significantly larger. Moreover, since explicit atomic vibrations are not followed, the timestep in the numerical integration is longer. One more advantage of the breathing sphere model is the ability to simulate complex multicomponent organic materials [10]. One can easily include bonding interactions, different strengths and absorptions of different components. The rate of energy transfer within an individual component as well as between components can be precisely controlled.

The effect of laser irradiation is simulated by vibrational excitation of random molecules during the time of the laser pulse within the penetration depth appropriate for a given wavelength. Vibrational excitation is modeled by depositing a quantum of energy equal to the photon energy into the kinetic energy of internal vibration of a given molecule. The absorption probability can be modulated by Beer's law to reproduce the exponential attenuation of the laser light with depth or can be restricted to a certain component within a complex material.

Owing to the approximations adopted in the breathing sphere model, computational cells can be large enough to reproduce the collective dynamics leading to laser ablation and damage. One effect, however, that can not be directly simulated within the MD model is propagation of the laser induced elastic wave. The method used to minimize the effects of the reflection of the wave from the boundary of the computational cell are discussed in the next section.

DYNAMIC BOUNDARY CONDITION

The generation of stress waves is a natural result of the fast energy deposition in the case of short pulse laser irradiation and inhomogeneous absorption [7,9,11]. This is illustrated in Figure 1 where the energy contour plots reflect the formation and propagation of a plane pressure wave within the MD computational cell. In this case the high pressure builds up during the 15 ps laser pulse within the penetration depth, 32 nm, of the irradiated sample. The high pressure contributes to the ablation of a part of the irradiated volume and drives a strong compression wave into the bulk of the sample. Simulation of the propagation of the pressure wave requires the size of the MD computational cell to be increased linearly with the time of the simulation. For times longer than ~100 ps the size of the model required to follow the wave propagation becomes computationally prohibitive and artificial border effects can interfere with the simulation results. Both rigid and free boundary conditions lead to the complete reflection of the pressure wave, as shown in Figure 1a. This reflection of the pressure wave can cause the effect known as back spallation [7,11], when the tensile strength of the material is exceeded and fracturing occurs at a certain depth near the back surface of the sample. The reflected wave can also reach the front surface of the irradiated sample and contribute to the material ejection.

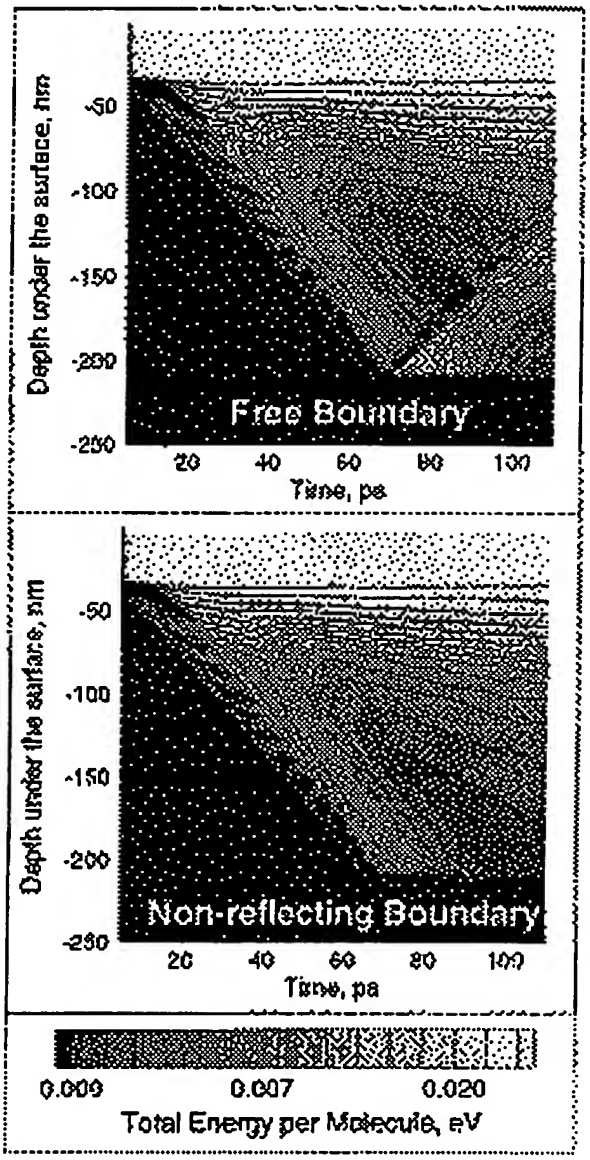

Figure 1: Energy contour plots for free and non-reflecting boundary condition applied at the bottom of the computational cell.

In order to avoid artifacts due to the pressure wave reflection, we have developed a simple and computationally efficient non-reflecting boundary condition based on analytical evaluation of the forces acting at the molecules in the boundary region from the outer "infinite medium" [7]. In this approach the boundary condition is a set of terminating forces that are applied to the molecules in the boundary region. In the calculation of the terminating forces, that are updated at each integration step, we take into account three effects, namely, the static forces that mimic interaction with molecules beyond the computational cell, the forces due to the pressure wave propagation

Technical Proceedings 1999 International Conference on Modeling and Simulation of Microsystems (MSM '99), Applied Computational Research Society, 1999.

through the boundary region, and the forces due to the direct laser energy absorption in and around the boundary region during the laser pulse.

As shown in Figure 2b, the dynamic boundary condition allows us to completely eliminate simulation artifacts associated with the reflection of the pressure wave from the boundary of the MD computational cell and to restrict area of the MD simulation to the region where active processes of laser induced melting, ablation and damage occur. In effect, this significantly expands the scope of phenomena that can be addressed and allows to use irradiation parameters comparable to the experimental values [12].

SIMULATION RESULTS

The mechanisms of laser ablation

In order to understand the basic processes leading to the material ejection, we performed a series of simulations of short pulse laser irradiation of a model molecular solid with a range of laser fluences. We found that there are two distinct regimes of molecular ejection separated by a well-defined threshold fluence. At fluences below threshold thermal desorption from the surface is observed, the desorption yield consists primarily of monomers, Figure 2a, and the desorption yield has an Arrhenius-type dependence on the laser fluence. At the threshold fluence the ejection mechanism changes from desorption to ablation, in which a collective ejection of a volume of irradiated material occurs. The change in the ejection mechanism manifests itself in more than an order of magnitude stepwise increase in the amount of ejected material, Figure 3, and in a drastic change in the plume composition. Large clusters become a major constituent of the plume above threshold, Figure 2b, and the total amount of ejected material follows the critical volume energy density deposited by the laser pulse[12]. The laser induced pressure buildup and the phase explosion due to overheating of the irradiated material are identified as the key processes responsible for material ejection in the ablation regime [5,6,12,13].

Total yield vs. yield of monomers

One important result from the simulations is an indication on a drastic difference in the fluence dependence of the total ablation yield and a yield of individual molecules, measured as a count rate in mass spectrometry experiments [12]. This difference is obvious from Figure 3 where both total yield and monomer yield are plotted. There is no step increase in the number of ejected monomers at the ablation threshold and one can hardly identify the threshold fluence from this dependence. An Arrhenius-type dependence of the monomer yield on fluence, albeit appropriate for the regime of thermal desorption only, appears to work over a larger fluence region, Figure 3. This observation provide an explanation for recent experimental results in MALDI [4]. Simulation

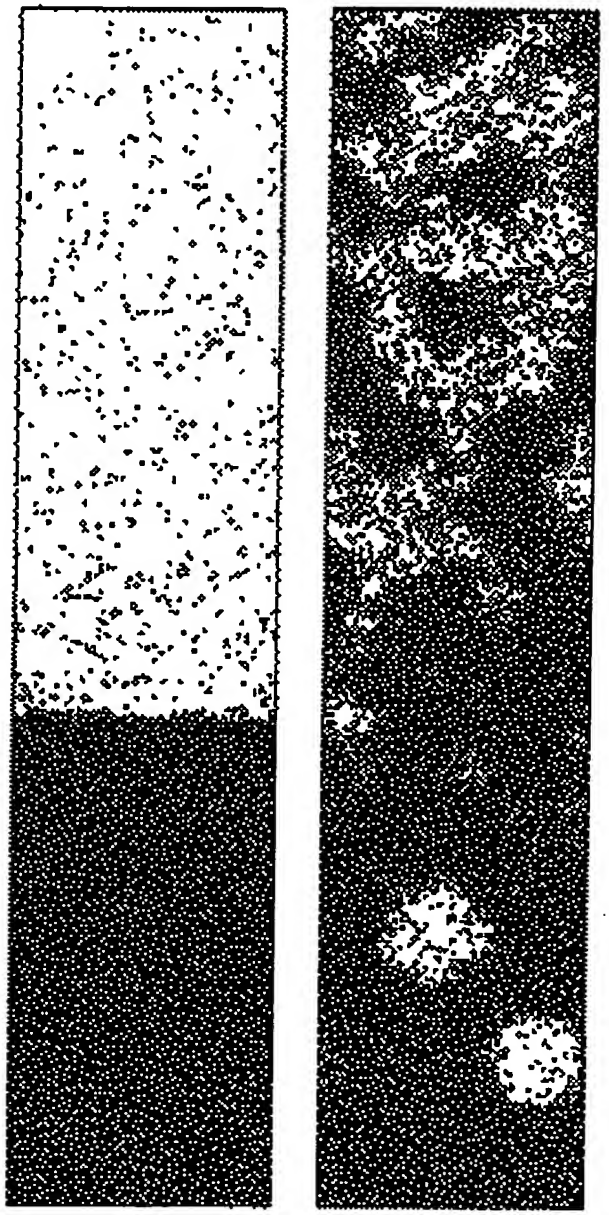

(a) (b)

Figure 2: Snapshots from the simulation of irradiation of molecular solid with 150 ps laser pulse at laser fluences of (a) 34 J/m^2 and 55 J/m^2.

results clearly demonstrate that the yield of individual molecules does not reflect in any quantitative extent the total amount of material ejected in the ablation regime. The difference in the physical mechanisms of molecular ejection below and above the ablation threshold leads to a drastically different plume composition and should be taken into account in order to provide an adequate analytical description of the yield vs fluence dependence in mass spectrometry experiments.

Technical Proceedings 1999 International Conference on
Modeling and Simulation of Microsystems (MSM '99),
Applied Computational Research Society, 1999.

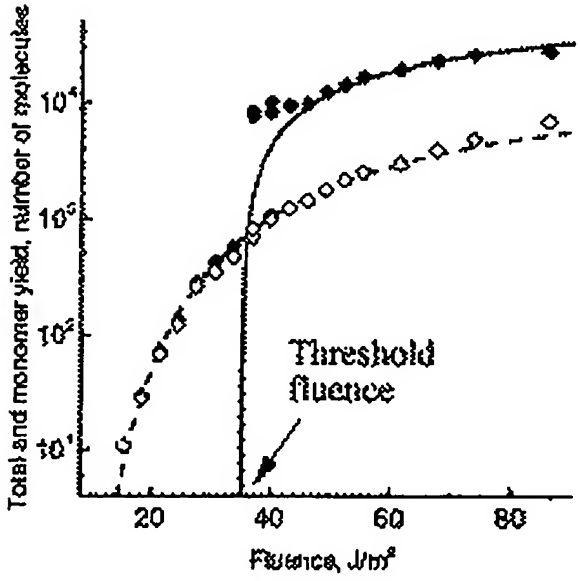

Figure 3: Total and monomer yield, vs. laser fluence. The solid line represent predictions of the ablation model (volume energy density criteria), the dashed line represents prediction of the thermal desorption model [12]. The closed and open symbols show the data points for total yield and monomer yield, respectively.

Other recent applications of the model include development of a consistent analytic description of the velocity distributions of matrix and analyte molecules in MALDI [14,15], analysis of the mechanisms of laser damage to spatially localized absorbers [10,16], and development of a combined molecular dynamics – finite element method for multiscale simulations [17].

SUMMARY

First results of the microscopic simulations of laser ablation and damage of organic solids demonstrate that with growing computer power and certain reasonable approximations it is now possible to apply the MD simulation technique for analysis of complex collective phenomena of laser ablation. Molecular-level simulations provide a comprehensive picture of the processes leading to ablation and damage both at mesoscopic level, in terms of energy, temperature and pressure development in the irradiated material, and at microscopic level, in terms of laser induced molecular motions. In effect, one has a unique opportunity to relate detailed information on the physical processes to experimentally observed results of laser irradiation.

ACKNOWLEDGMENTS

This work was supported by the NSF Chemistry Division and the ONR through the MFEL Program. The computational support for this work was provided by the IBM-SUR Program and the Center for Academic Computing at PSU.

REFERENCES

[1] *Laser Ablation and Desorption*, edited by J. C. Miller and R. F. Haglund, Jr., Academic Press, 1998.

[2] Proceedings of the 4th International Conference on Laser Ablation, edited by R. E. Russo, D. B. Geohegan, R. F. Haglund, K. Murakami, Appl. Surf. Sci. **127-129**, 1998.

[3] *Laser - Tissue Interaction IX*, edited by S. L. Jacques, SPIE Proceedings Series **3254**, 1998.

[4] K. Dreisewerd, M. Schürenberg, M. Karas, and F. Hillenkamp, Int. J. Mass Spectrom. Ion Processes **141**, 127-148, 1995.

[5] L. V. Zhigilei, P. B. S. Kodali, and B. J. Garrison, J. Phys. Chem. B **101**, 2028-2037, 1997.

[6] L. V. Zhigilei, P. B. S. Kodali, and B. J. Garrison, J. Phys. Chem. B **102**, 2845-2853, 1998.

[7] L. V. Zhigilei and B. J. Garrison, in Multiscale Modelling of Materials, edited by T. Diaz de la Rubia, T. Kaxiras, V. Bulatov, N. M. Ghoniem, and R. Phillips, (Mater. Res. Soc. Proc. **538**) in press, 1999.

[8] R. E. Wyatt, C. Iung, and C. Leforestier, Acc. Chem. Res. **28**, 423-429, 1995.

[9] H. Kim and D. Dlott, J. Chem. Phys. **94**, 8203-8209, 1991.

[10] L. V. Zhigilei and B. J. Garrison, in Ref. 3, 135-143, 1998.

[11] G. Paltauf and H. Schmidt-Kloider, Appl. Phys. A **62**, 303-311, 1996.

[12] L. V. Zhigilei and B. J. Garrison, Appl. Phys. Lett. **74**, in press, 1999.

[13] L. V. Zhigilei, P. B. S. Kodali, and B. J. Garrison, Chem. Phys. Lett. **276**, 269-273, 1997.

[14] L. V. Zhigilei and B. J. Garrison, Appl. Phys. Lett. **71**, 551-553, 1997.

[15] L. V. Zhigilei and B. J. Garrison, Rapid Commun. Mass Spectrom. **12**, 1273-1277, 1998.

[16] L. V. Zhigilei and B.J.Garrison, Applied Surface Science **127-129**, 142-150, 1998.

[17] J. A. Smirnova, L. V. Zhigilei, and B. J. Garrison, Comput. Phys. Commun., in press, 1999.

[18] More information on the project can be found at http://galilei.chem.psu.edu/~leo/Ablation.html